AD-A130 398 EXPERIMENTAL MEASUREMENTS OF WAKE CHARACTERISTICS OF LOW ASPECT-RATIO DELTA AND FLAPPED-PLATE PLANFORMS(U) AIR FORCE ACADEMY CO C R KEDZIE ET AL. 15 MAR 83 1/1

UNCLASSIFIED USAFA-TN-83-6 F/G 20/4 NL

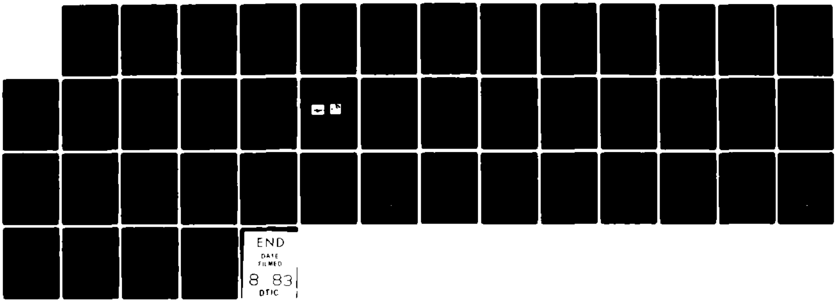

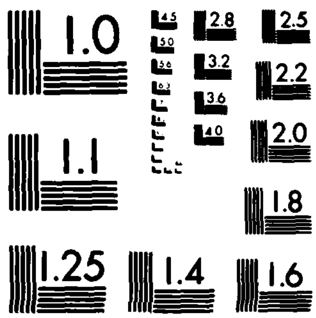

MICROCOPY RESOLUTION TEST CHART
NATIONAL BUREAU OF STANDARDS-1963-A

(12)

USAFA-TN-83-6

Department of Aeronautics
Dean of the Faculty
United States Air Force Academy
Colorado 80840

EXPERIMENTAL MEASUREMENTS OF WAKE CHARACTERISTICS OF LOW ASPECT-RATIO DELTA AND FLAPPED-PLATE PLANFORMS

TECHNICAL NOTE
USAFA-TN-83-6

Kedzie, C.R.

Griffin, K.E.

15 MARCH 1983

Any views expressed in this paper are those of the author. They should not be interpreted as reflecting the views of the USAF Academy or the official opinion of any governmental agency. Notes are not reviewed for content or quality by the USAF Academy but are published primarily as a service to the faculty to facilitate internal research communication.

This Technical Note has been cleared for open publication and/or public release by the appropriate Office of Information in accordance with AFR 190-17 and DODD 5230.9. There is no objection to unlimited distribution of this Technical Note to the public at large or by DDC to the National Technical Information Service.

Thomas E. McCann, Lt. Colonel, USAF
Director of Research and Continuing Education

FORWARD

This technical note is a report on the forward-swept wing research conducted by the Aeronautics Laboratory at the United State Air Force Academy during the period from 1 Jan 82 to 1 June 82. This technical effort was sponsored by the Defense Advanced Projects Agency (DARPA) and administered as ARPA 4364 by Col James Allburn. Capt K.E. Griffin, the principal investigator, was assisted by the staff and cadets at the Air Force Academy.

The report documents the wake locations and velocity fields of two low aspect-ratio lifting surface planforms, a bent plate and a delta. The bent plate represents a low aspect-ratio wing with a deflected flap at the 50 percent chord line. The delta is typical of high-speed planforms and strake configurations. The wake characteristics and locations measured in this paper can be used to correlate the new theoretical lifting surface/wake prediction methods using experimental wake data. The velocity field plots are useful in interpreting the velocity field in and around the wakes and the wake movements streamwise.

EXPERIMENTAL MEASUREMENTS OF WAKE CHARACTERISTICS
OF LOW ASPECT-RATIO DELTA AND FLAPPED-PLATE PLANFORMS

C.R. Kedzie* and K.E. Griffin**

Abstract

This report documents the characteristics and location of the wakes for two generic lifting surface planforms. The geometric description locates these wakes as they develop downstream from a low aspect-ratio delta wing and a bent-plate wing. The wakes are graphically depicted at several streamwise locations downstream of these wings with accompanying cross-velocity vector plots to assist in interpreting them. The data used to determine these wake characteristics was obtained by surveying the wings' flow field with a seven-hole pressure probe.

I. Introduction

For this research effort, a seven-hole pressure probe was employed to measure the wakes produced by two simple planform shapes: a low aspect-ratio flat plate with a 50 percent chord flap deployed 20 degrees and a low aspect-ratio delta wing. These planforms were tested at low speeds and moderate angles-of-attack to study their wake characteristics. In the past these planforms have been employed to demonstrate lifting surface wakes using such flow visualization techniques as the water table and dye methods described in Ref. 1. These demonstration methods, however, are applicable only to low Reynolds numbers and give only qualitative visualizations. The following data represents not only flow visualizations at higher Reynolds numbers (where the vortex systems exhibit a great deal of the turbulence that is characteristic of flight vehicle

*Cadet, USAF Academy
**Captain, USAF Academy, Associate Professor of Aeronautics, DFAN

lifting surfaces) but also the freestream pressure and velocity values. The planforms analyzed in this paper have been used in the development of analytical prediction methods for lifting surface wakes, such as those found in Ref. 2. These analytical methods typically use mathematical singularities arrayed in the freestream math model wake to refine the lifting surface flow predictions. The experimental values of pressure and velocity reported here can be used to provide wake locations and downwash velocity values for correlation with the analytical predictions of these planforms.

The first planform configuration is shown in Figure 1. The mid-chord bend in this low aspect-ratio lifting surface places the downstream portion of the plate at a 20 degree angle to the upstream portion. The lifting surface angle-of-attack is defined by the upstream half of the plate, with the downstream portion treated as a large trailing edge flap.

This bent-plate configuration is interesting because of the flow structure of the tip vorticity. The discontinuity in slope at the mid chord produces a sharp change in the vortex created at the wing tip. In fact, when very low Reynolds number experiments with this model are observed, a well-defined vortex core appears streamwise at this bend location. This vortex becomes embedded in the wake that is wrapped around the core of the wing tip vortex. This small vortex core caused by the bend provides a pressure characteristic in the tip vortex system that can be observed at various downstream locations. Its rotary position

about the tip vortex core, as progressively more downstream locations of the tip vortex system are observed, defines the rotation rate developed in the tip vortex system.

The second planform configuration is shown in Figure 2. This highly-swept delta configuration produces a leading edge/tip vortex system similar to that observed around the strakes of modern fighter aircraft. This vortex system builds in strength when moving streamwise along the leading edge; downstream, it wraps the trailing edge wake up and in towards the centerline of the model. Since modern fighter configurations use this strake vortex to delay flow separation over their primary wings, the location and strength of this type of lifting surface vortex system is critical.

II. Background

The Aeronautics Laboratory of the USAF Air Force Academy has developed an experimental technique that can measure, in freestream flow, pressure and velocity information from steady fields even with highly irregular flows. The test technique uses a multi-port pressure probe linked to a computer system that produces real-time flow field data for any geometric location in which the pressure probe tip can be positioned. This particular seven-hole pressure probe was first developed to measure incompressible flow at the Air Force Academy under the sponsorship of the NASA Ames Research Laboratory (Ref. 3). The probe capabilities were later expanded to include supersonic

capability (Ref. 4). This probe is being used in ongoing research efforts to experimentally document lifting surface wakes, particularly those of the X-29 Forward-Swept Wing Flight Demonstrator. The first wake survey in which the seven-hole probe was used studied a generic canard/swept-wing configuration (Ref. 5). The present study of the delta and bent-plate planforms provides background information on lifting surface wake formations that will be used later in an in-depth investigation of the canard/wing wake interactions of a 1/10 scale model of the X-29 Forward-Swept Wing Demonstrator Aircraft.

The seven-hole pressure probe used for these wake studies is shown in Figure 3. Its small size (.109 inches in diameter) gives the probe the ability to move inside the near flow fields of wind tunnel models of moderate size without significantly disturbing that flow field. The position of the probe is maintained by an automated device or traverse. The traverse locates the probe anywhere in the test section by coordinate locations relative to a test section coordinate origin preselected at the beginning of the test. This positioning traverse also allows the wind tunnel computer to be used to specify probe locations using selected arrays of data point coordinates.

The probe is made up of a central pressure port located normal to the centerline of the probe. It is surrounded by six pressure ports on the conical face of the probe. These seven pressure ports are connected to electronic pressure transducers

by tubing having a very small diameter. With these transducers providing electrical analogs to the pressures, a computer can be used to interpret directly the digitized values of raw pressure at these port locations.

The technique used to infer flow field pressures and velocity from the raw pressure values measured at these seven pressure ports involves seven sets of fourth-order polynomial equations. These equations, along with the non-dimensionalized forms of their coefficients, are presented in Ref. 4. The coefficients are established by calibration tests at known flow conditions and remain stored in a data acquisition computer for use with unknown flow fields. Using the raw pressure data from the seven-hole probe these equations, with their calibrated coefficients, provide a means of calculating the more useful values of total, static, and dynamic pressures and velocity vectors at any selected point in the flow. The pressure and velocity values for each data point are recorded on high-speed disk storage for later use in developing the lifting surface flow field interpretations.

The data points for the tests are arranged in planes having common streamwise coordinates. This facilitates both data acquisition and presentation. The planes are chosen at various streamwise locations as measured from the trailing edge of each model. By locating the wake characteristics at each streamwise position in the flow, one can observe and interpret their development as the flow proceeds.

With a complete set of pressure and velocity data stored for each data point, velocity vector and pressure contour plots in the data planes can be quickly generated as testing proceeds. This ensures that all of the important locations in the flow field are surveyed in each data plane. Later these plots can be used to locate important flow characteristics such as vorticity, wakes, and downwash for final interpretation of the lifting surface wakes.

Figure 4 is a sample cross-velocity flow field data plot generated with data taken from the bent plate at 20 degrees angle-of-attack. This figure shows the cross-velocity vectors at the data points surveyed on the data plane immediately downstream of the trailing edge of the bent plate. These vectors represent the projection on the data planes of the total velocity vector that was measured at each data point. Their origins give the geometric location of the data points, their length gives the relative magnitude of the in-plane velocity components, and their arrow heads depict the flow directions.

In Figure 4 the view is looking upstream about the port side wing, and the cross-velocity vectors indicate a strong clockwise swirling motion (typical of a streamwise vortex) that is centered at about 1.6 inches in the negative x direction and 1.8 inches in the positive y direction. The direction of rotation in the cross flow is that expected about the tip vortex generated by positive lift on the port wing. The center of this motion will then be the core filament of the vortex. The locations and relative

strengths of vortex systems, as well as the general downwash flow field directions, can be determined by these velocity fields.

Pressure contour plots complement those containing the cross-velocity vectors and can be most useful in wake location calculations. In Figure 5 the total pressure coefficient contours are shown for the same data points viewed in the same direction as in Figure 4. This total pressure coefficient is defined by total pressure comparisons between local and freestream conditions.

$$\Delta C_{P_o} = \frac{P_{o_{Local}} - P_{o_{Tunnel}}}{P_{o_{Tunnel}} - P_{\infty_{Tunnel}}} \qquad (1)$$

The difference between local ($P_{o_{Local}}$) and freestream ($P_{o_{Tunnel}}$) total pressure is nondimensionalized by the freestream dynamic pressure. As irreversible losses in total pressure occur locally, due to viscosity in large velocity gradient regions, C_{P_o} becomes negative. These velocity gradient regions occur near the core of vortex filaments and in the boundary layers of lifting surfaces. This loss in total pressure provides a signature in downstream flow that can be used to identify their freestream wake locations.

In Figure 5 contours of various values of C_{P_o} indicate regions where losses in total pressure have occurred. Note that the wake of the plate can be seen in the pressure values. The way this wake wraps around the tip vortex core is shown downstream of the tip chord of the plate. Using contour plots like Figure 5 the wak‹ locatio⁻ ı and the vortex systems at their

edges have been determined for both the plate and delta planforms in each data plane. The plots of their wake locations are found at the end of this report.

III. Test Apparatus

The two planforms were tested in the subsonic continuous flow wind tunnel of the Aeronautics Laboratory at the USAF Academy. The test section is two feet by three feet in cross section, with the freestream velocity maintained for this test at 100 feet per second.

The bent-plate model of Figure 1 was mounted on a thin vertical strut from the tunnel ceiling. The two model attitudes used in developing the following data were angles-of-attack of 10 and 20 degrees with respect to the freestream direction (as measured from the forward half of the model). The unit normals of the planes that define the data point streamwise locations were always parallel to the freestream direction.

The delta planform model was also run at 10 and 20 degree angles-of-attack. Again, the unit normals of the planes used to organize the data points were parallel to the freestream direction.

IV. Results

The data obtained for the two planforms is presented graphically. For each set of data points, a cross velocity plot is presented, followed by a second plot showing the intersection

of the plane containing those points with the lifting surface wake. The wake is plotted from the centerline outboard, showing the way it becomes wrapped in the tip vorticity until its pressure signature cannot be distinguished from the inner field of the tip vorticity. The core location of the tip vortex is also noted. If the data plane intersects the wing planform, this is also noted. The streamwise development of the wake for different wing angles-of-attack can be compared for both planforms.

A. Bent-Plate Results

The bent plate data is taken from the centerline towards the port side of the plate. Since all flow configurations are symmetric about a vertical plane passing through the planform centerline, the flow field of only one side of the planform is presented to allow greater detail in the plots. The coordinate system used for all the data points has its origin at the intersection of the vertical plane of symmetry with the trailing edge of the plate. The vertical direction (perpendicular to the freestream velocity vector) up (the positive lift side) from the plate is the positive y coordinate. The lateral direction (perpendicular to both the freestream direction and the y direction) is positive towards the starboard wingtip and is designated the positive x direction. All the plots are presented in such a way that the freestream velocity vector is out of the data plane. Thus the plots are to be viewed as looking upstream.

The data planes for 10 degrees angle-of-attack have streamwise locations relative to the trailing edge origin of -2, .2, 2, 4, 6, 9, and 12 inches. The data planes for 20 degrees angle-of-attack have locations of -2, .2, 2, 4, 6, and 11.5 inches. The data is presented in the planes in progressive streamwise locations with the cross-velocity vector plot followed by the wake location for each plane.

Figures 6 through 19 show the location and velocity fields of the wake and vortex core for the bent plate at 10 degrees angle-of-attack. Figures 20 through 31 show the same at 20 degrees angle-of-attack. For both angles-of-attack and any streamwise location, the x location for the vortex core remains approximately -1.5 inches. There are, however, changes in the y location of this vortex core.

The tip vortex core location in the y direction is influenced by the direction and strength of the downwash from the lifting surface. The downwash field -- and therefore the movement of the vortex core in the downwash direction -- is stronger at 20 degrees angle-of-attack than at 10 degrees. This is evident when one compares the locations of the tip vortex core in Figures 15 and 29 or Figure 19 and 31.

B. Delta Planform Results

The results of the low aspect-ratio delta wing planform tests are presented in Figure 32 through 55. Again, the data points lie above and in the wake of the port side of the wing.

The same coordinate system is used for the delta planform as was used for the bent plate, with the origin at the centerline trailing edge location of the delta planform.

The data planes for 10 degrees angle-of-attack have streamwise locations relative to the trailing edge origin of -2, .2, 2, 4, 6, 9, and 12 inches. The data planes for 20 degrees angle-of-attack have streamwise locations of -2, .2, 2, 4, and 6 inches. The plots of the wake locations and cross-velocity vectors for each plane of data points are presented in progressive streamwise fashion to indicate the movement of the wake as it travels downstream from the delta wing.

The delta wing results at 10 degrees angle-of-attack are contained in Figures 32 through 45. The results at 20 degrees angle-of-attack appear in Figures 46 through 55. The highly-swept leading edge develops a strake-like vortex system that travels in both the spanwise and downwash directions as progressively downstream data planes are surveyed. The downwash velocity vectors can be seen in each data plane cross velocity vector plot. Note the clockwise rotation of the port side leading edge vortex system. This is consistent with the positive lift condition created at 10 degrees angle-of-attack. Similar trends, only stronger, are found at 20 degrees.

The tip vortex core appears to seek the same locations at either 10 or 20 degrees angle-of-attack. This location is approximately -2.3 inches on the x axis and .2 inches on the y axis. This location for the tip vortex core appears to have been

achieved for both angles-of-attack in the data plane six inches downstream of the trailing edge.

The shape of the delta wing's downstream wake differs from that of the bent plate. Downstream of the delta trailing edge the portion of the wake that becomes wrapped around the vortex core is spread in a looser spiral than that found on the bent plate. This is especially noticeable in the x locations of the outboard wake that is wrapping around the core.

V. Conclusions

The low aspect-ratio delta wing demonstrates wing wake sensitivities to leading edge sweep. The leading edge sweep of the planform significantly affects both the way the wake becomes wrapped around the lifting surface tip vortex system and the movement of the vortex system downstream. With large leading edge sweep the wake bulges in a more spanwise fashion. Also, the tip vortex moves spanwise due to sweep effects but tends to find about the same downstream location relative to the delta wing trailing edge regardless of moderate values in angle-of-attack.

The bent-plate configuration addresses camber effects on wake characteristics using the 20-degree bend at mid chord. The secondary vortex system caused by the discontinuous slope change at the mid chord of the bent plate could not be discerned in the pressure data. This is due to the turbulence of the interior vortex flow field. The wake strength tended to determine the downstream vortex core location within the downstream range

available in this test for the unswept leading edge of the bent plate. Very little drift outboard was noted regardless of plate angle-of-attack.

The actual pressure and velocity values for each data point in these test cases (recorded on magnetic tape) can be obtained by contacting the Director of the Aeronautics Laboratory, Department of Aeronautics, USAF Academy.

References

1. Wickens, R.H., "The Vortex Wake and Aerodynamic Load Distribution of Slender Rectangular Wings," Canadian Aeronautics and Space Journal, June 1967.
2. Clark, D.R., Wathman, J.K., and Dvorak, F.A., "Forward Swept Wing Configuration Evaluation and Validations of Analytic Methods," AFWAL-TR-82-3033, July 1982.
3. Crandall, R. and Sisson, G., "Canard Wake Measurement and Description," Aeronautics Digest, USAFA-TR-81-4, USAF Academy, May 1981.
4. Gerner, A. and Sisson, G., "Seven-Hole Probe Data Acquisition System," USAFA-TN-81-8, Nov 1981.
5. Griffin, K.E., "Measurement of Wake Interactions of a Canard and a Forward Swept Wing," USAFA-TN-82-4, July 1982.

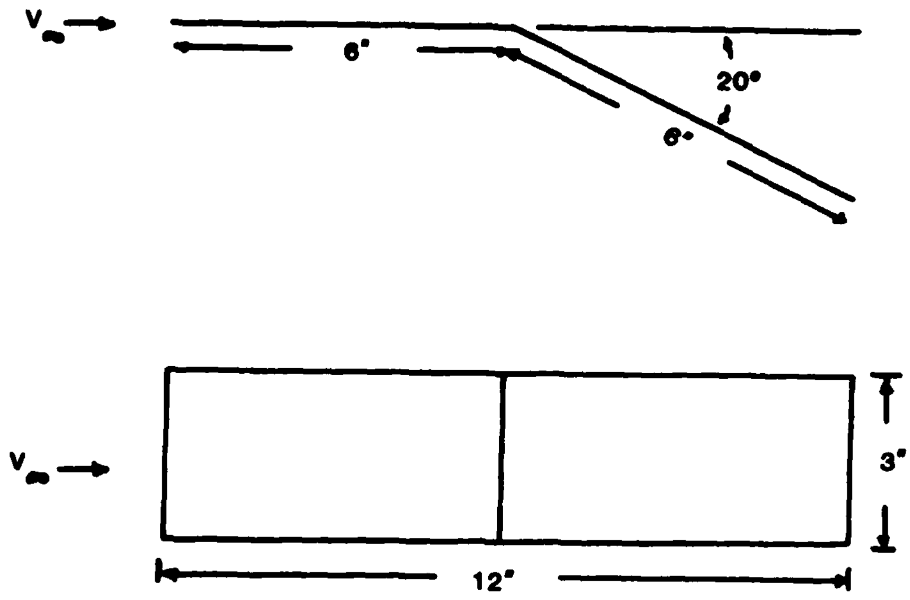

Figure 1. Model Geometry for Bent Plane

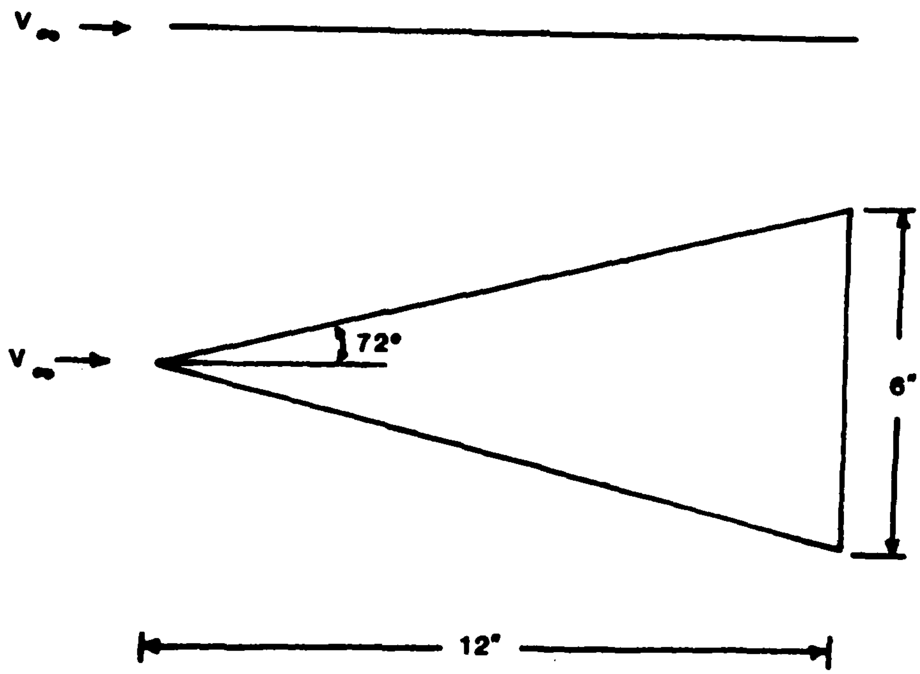

Figure 2. Model Geometry for Delta Plane

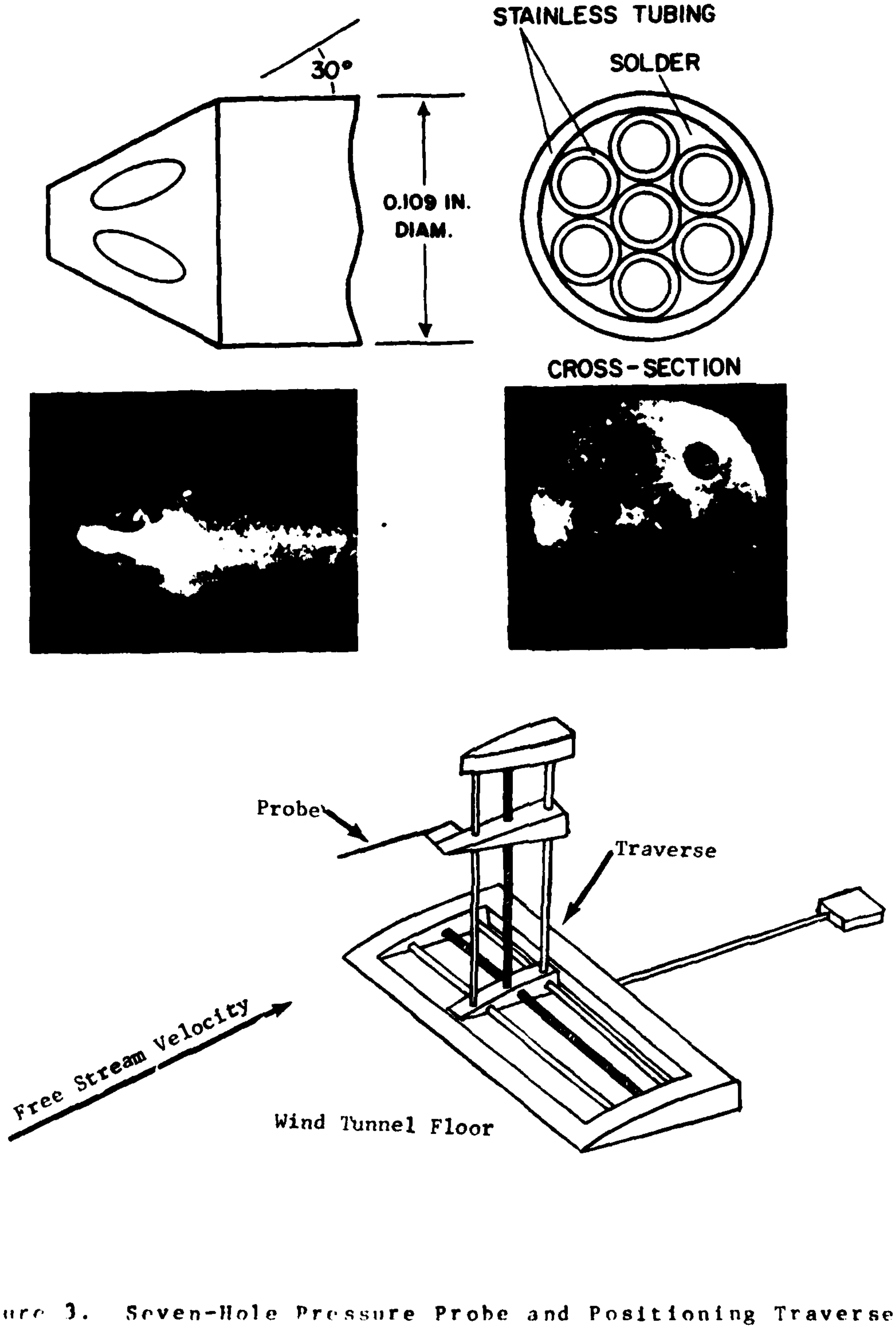

Figure 3. Seven-Hole Pressure Probe and Positioning Traverse

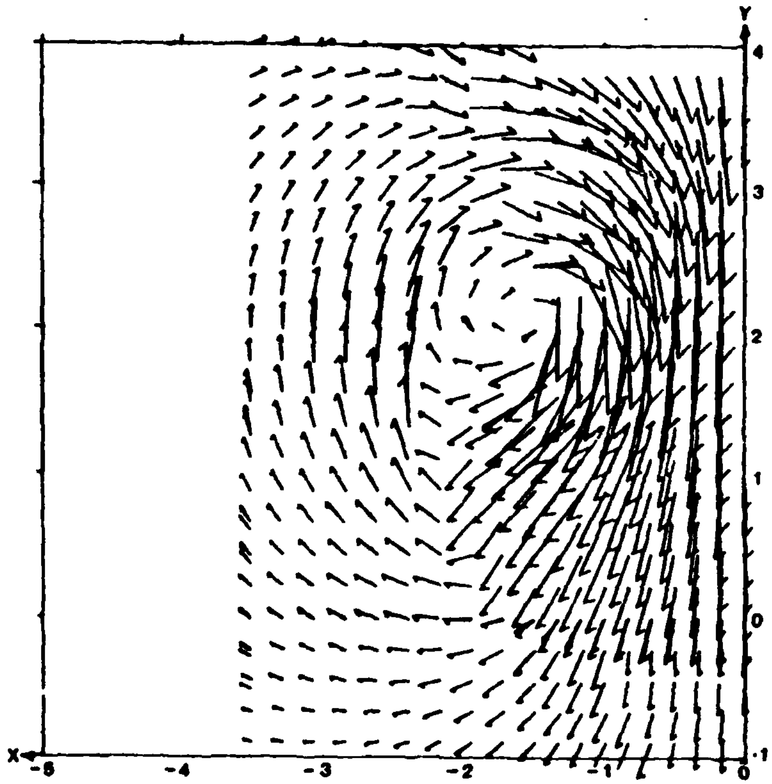

Figure 4. Example of Cross Velocity Vector Plot

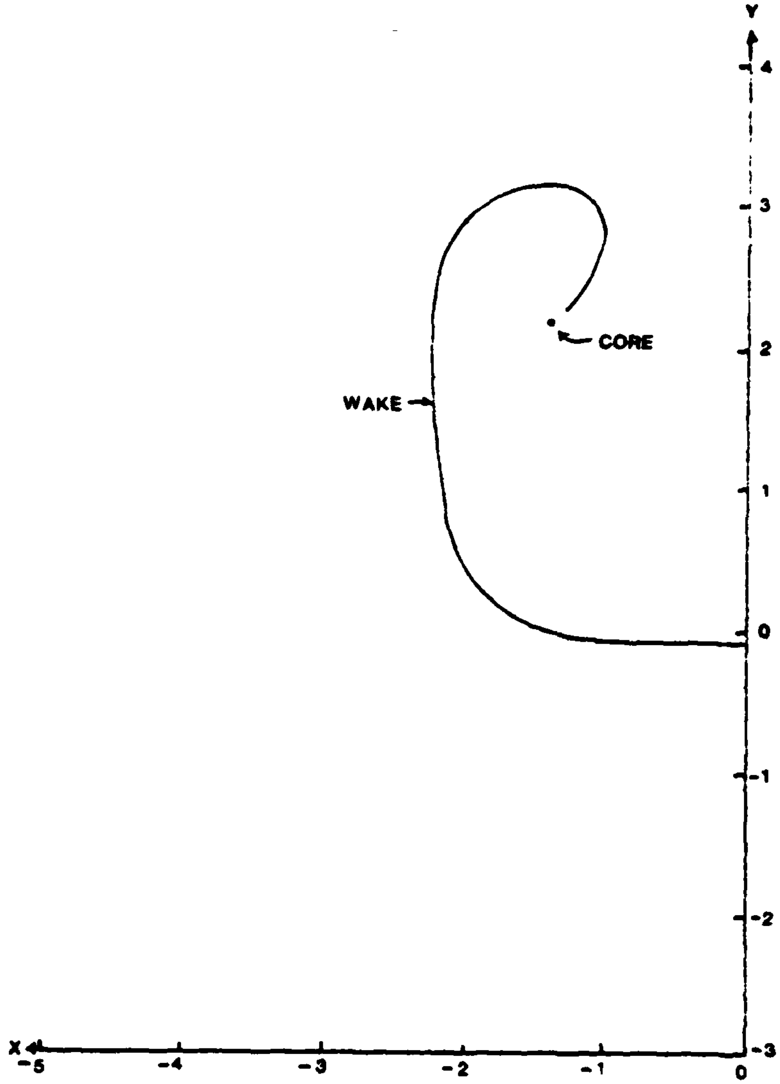

Figure 5. Example of C_{P_o} Plot

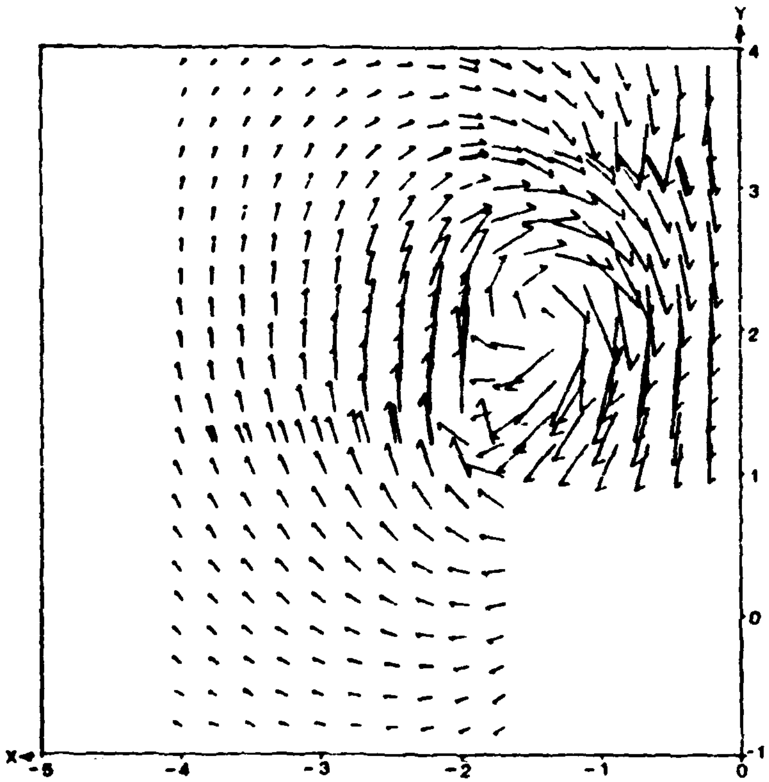

Figure 6. Bent Plate Cross Velocity Vector Plot, α = 10° and 2 Inches Upstream

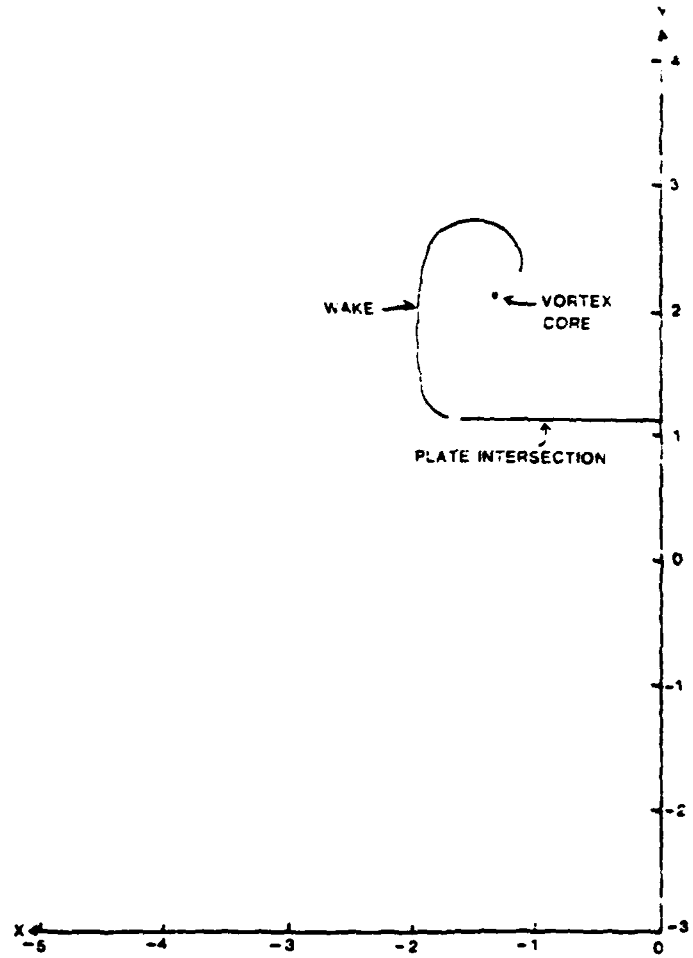

Figure 7. Bent Plate Wake Location, α = 10° and 2 Inches Upstream

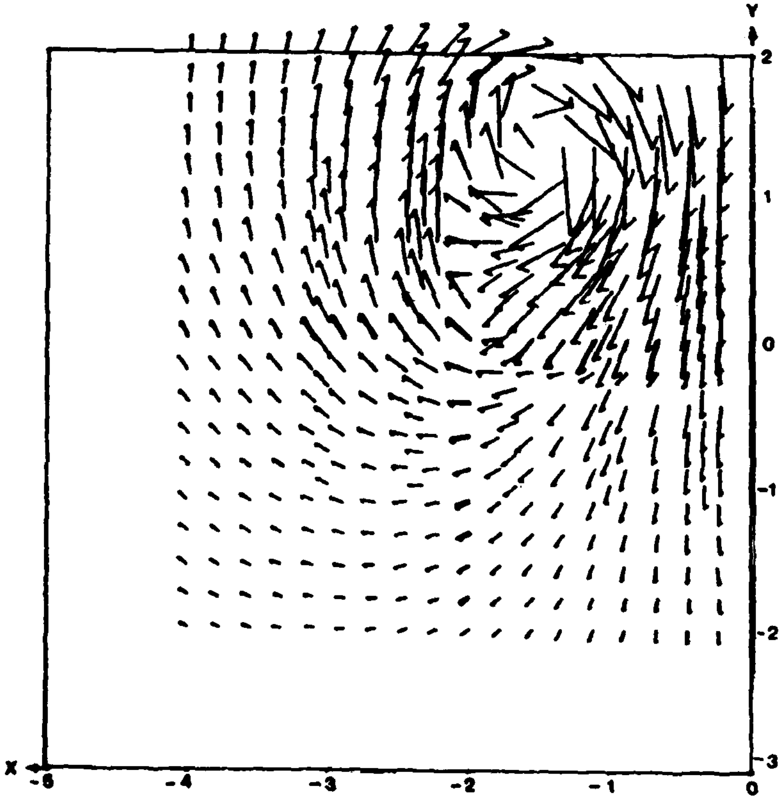

Figure 8. Bent Plate Cross Velocity Vector Plot, α = 10° and .2 Inches Downstream

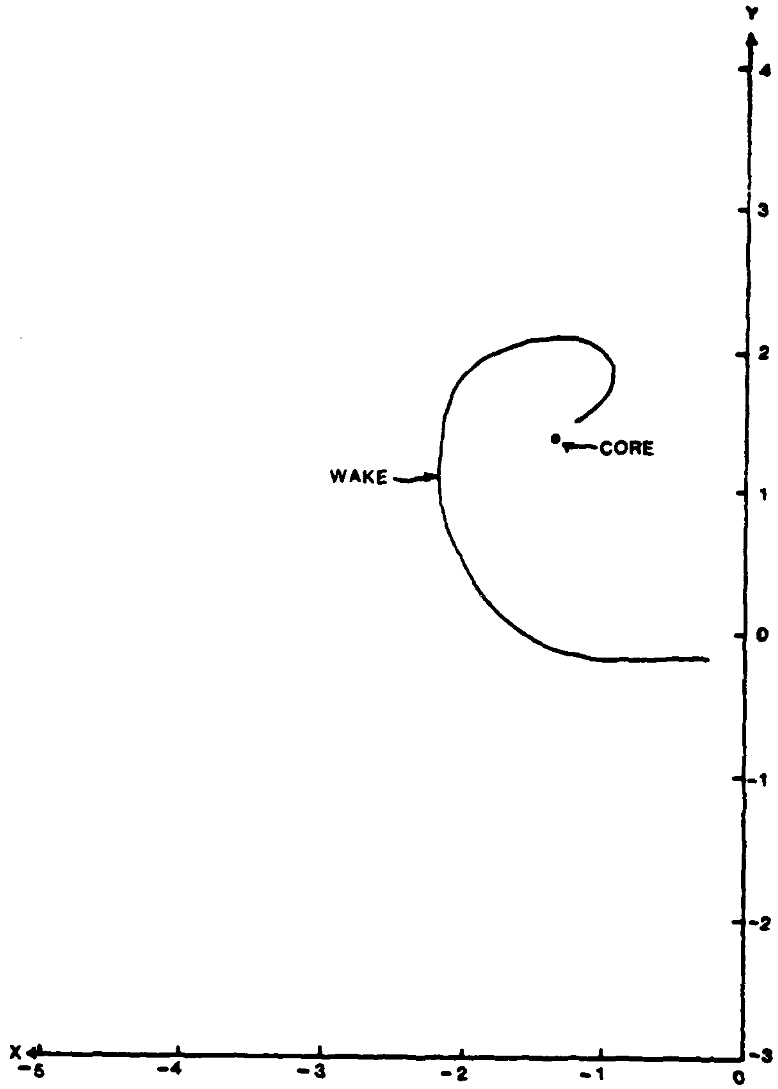

Figure 9. Bent Plate Wake Location, α = 10° and .2 Inches Downstream

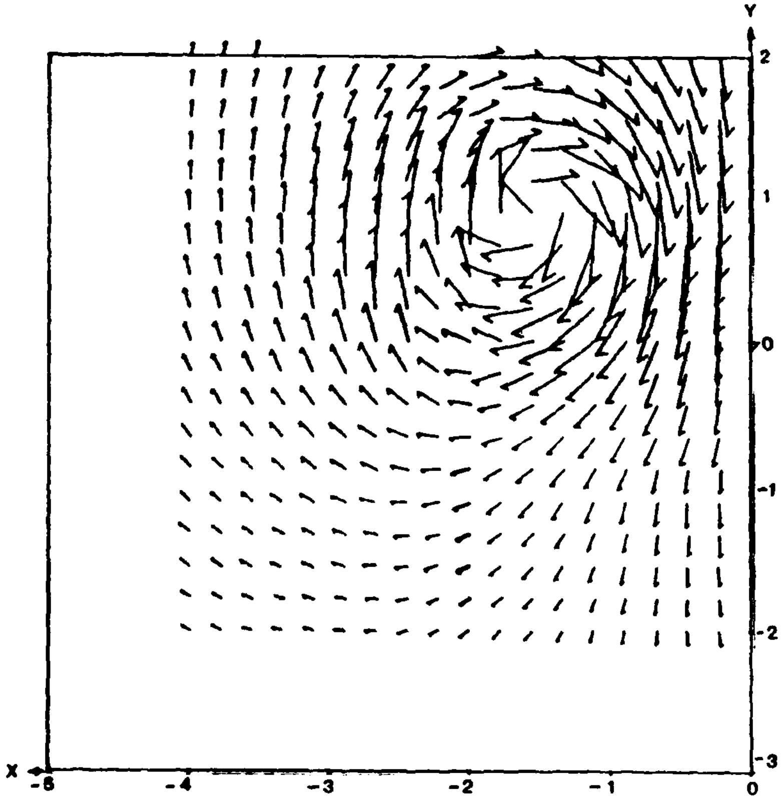

Figure 10. Bent Plate Cross Velocity Vector Plot, $\alpha = 10°$ and 2 Inches Downstream

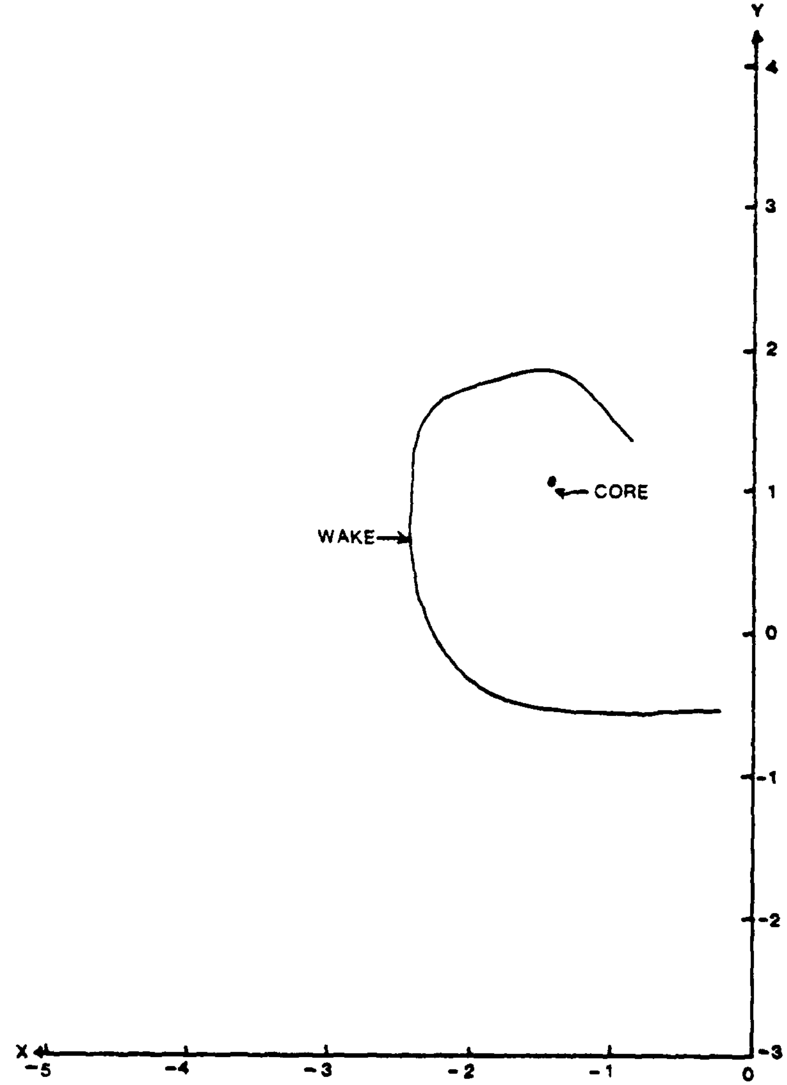

Figure 11. Bent Plate Wake Location, $\alpha = 10°$ and 2 Inches Downstream

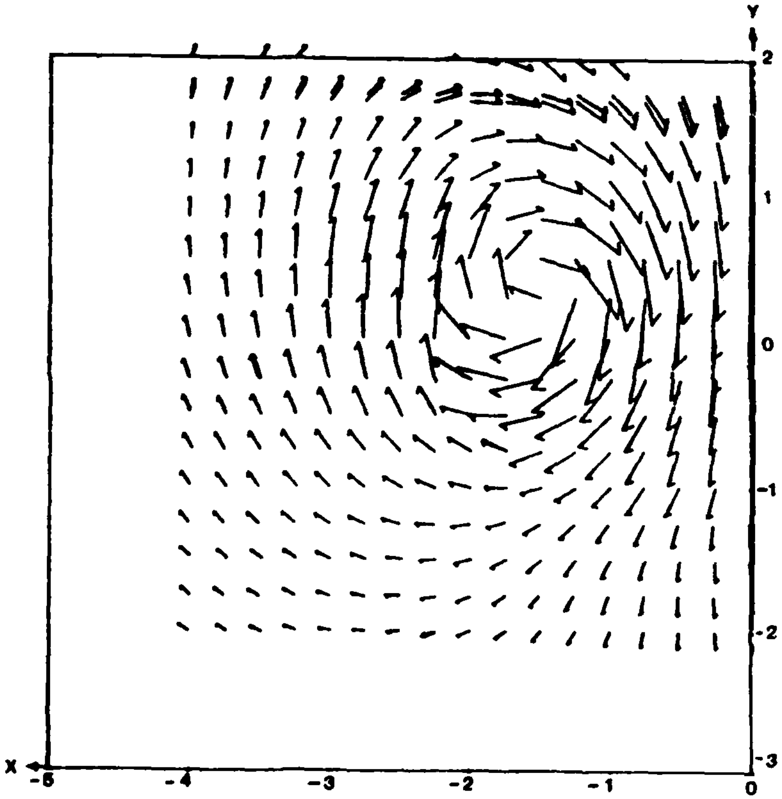

Figure 12. Bent Plate Cross Velocity Vector Plot, α = 10° and 4 Inches Downstream

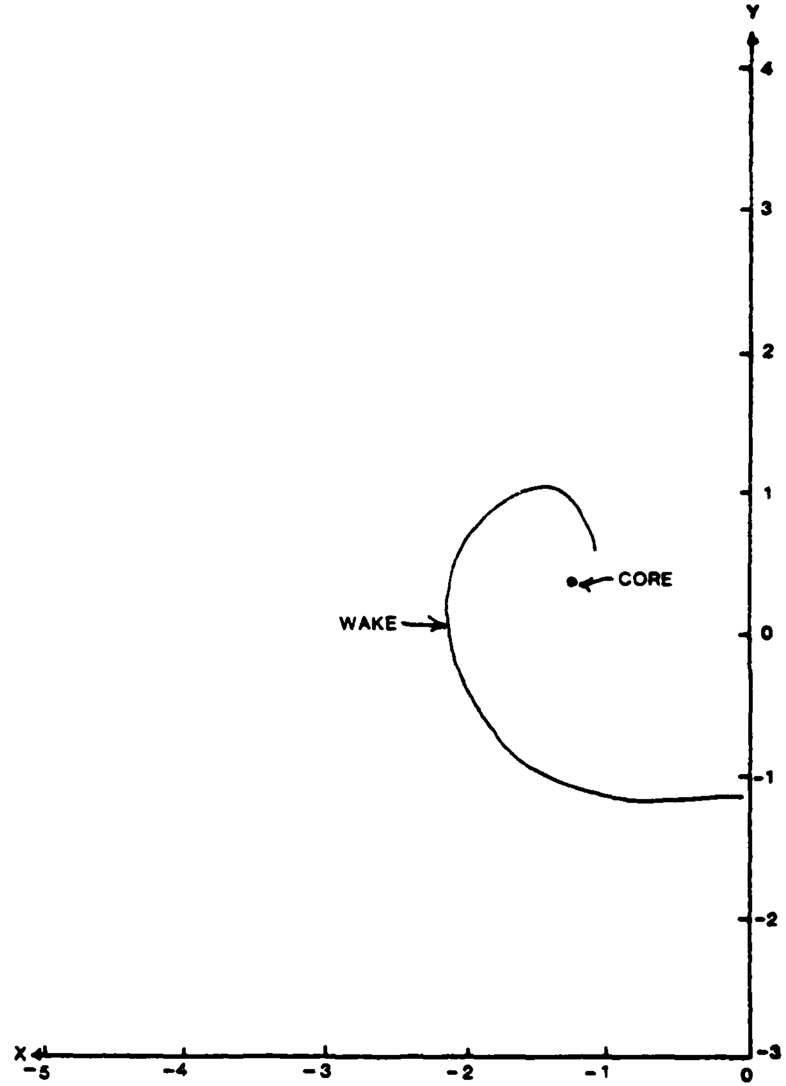

Figure 13. Bent Plate Wake Location, α = 10° and 4 Inches Downstream

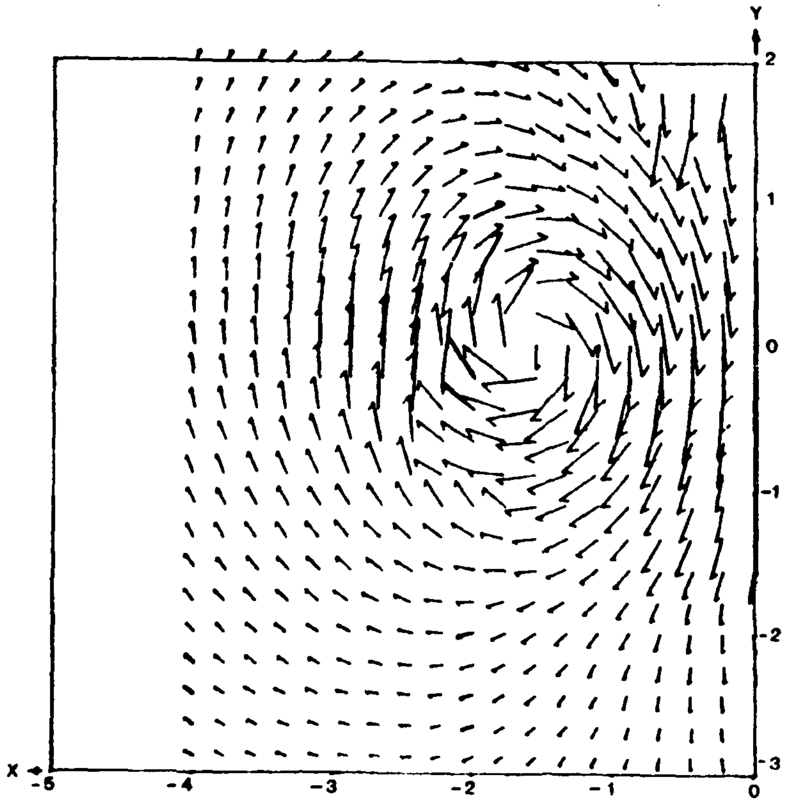

Figure 14. Bent Plate Cross Velocity Vector Plot, α = 10° and 6 Inches Downstream

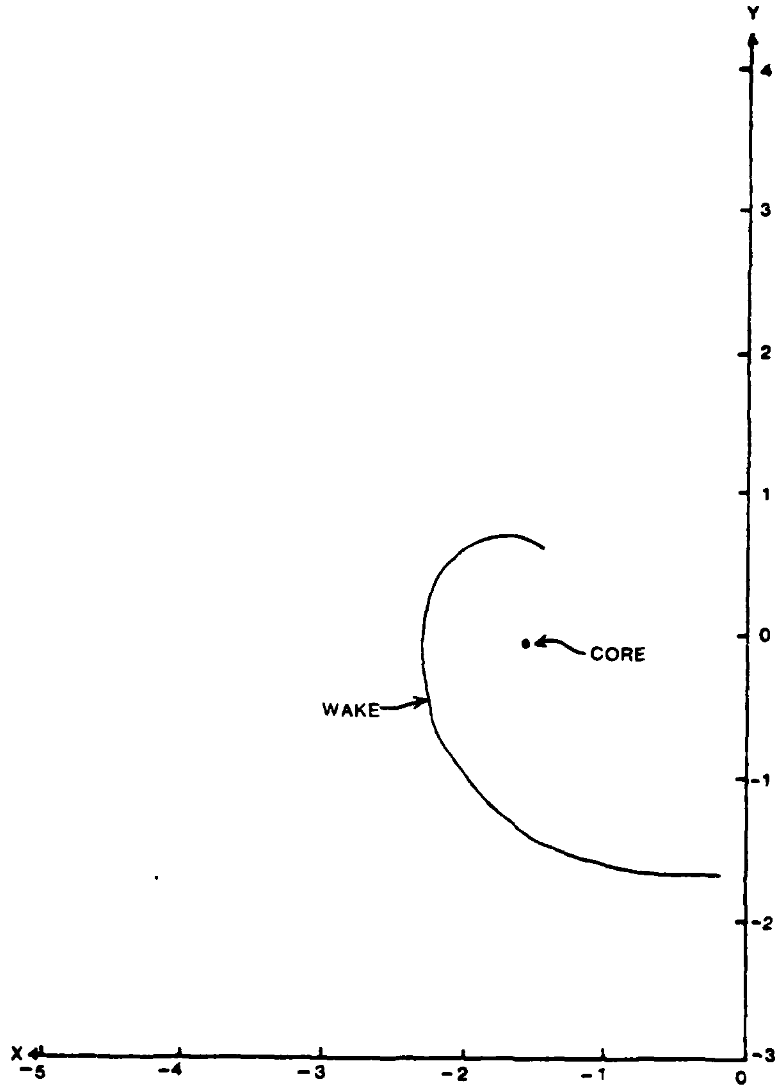

Figure 15. Bent Plate Wake Location, α = 10° and 6 Inches Downstream

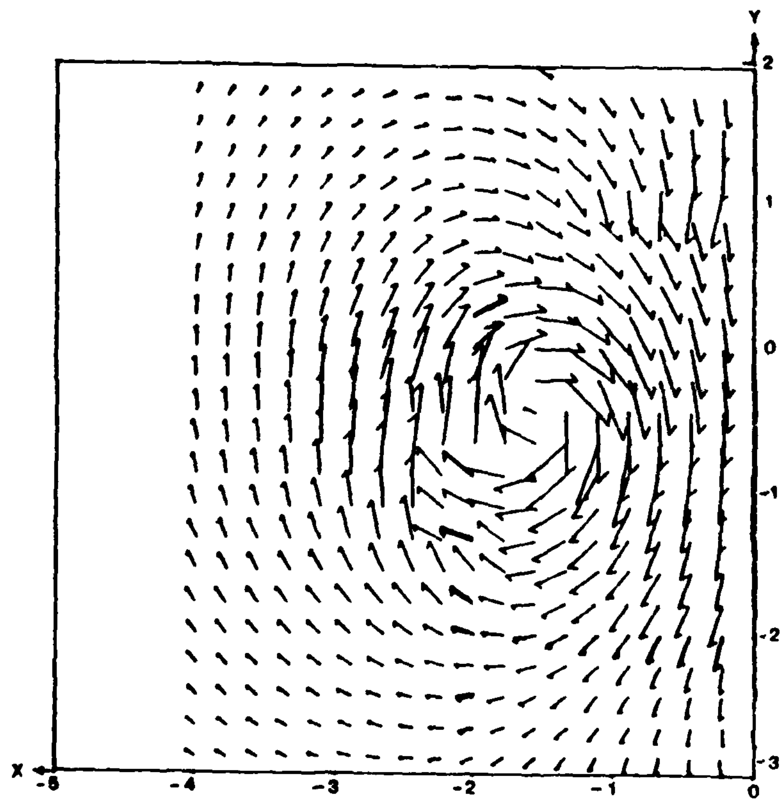

Figure 16. Bent Plate Cross Velocity Vector Plot, α = 10° and 9 Inches Downstream

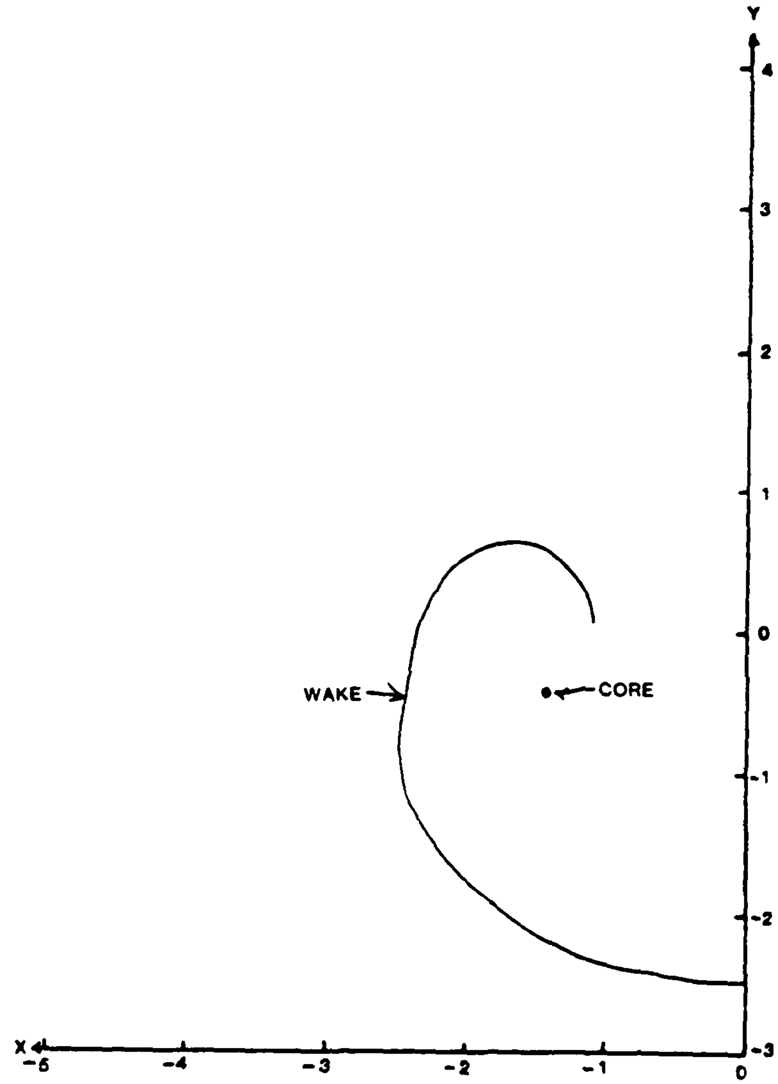

Figure 17. Bent Plate Wake Location, α = 10° and 9 Inches Downstream

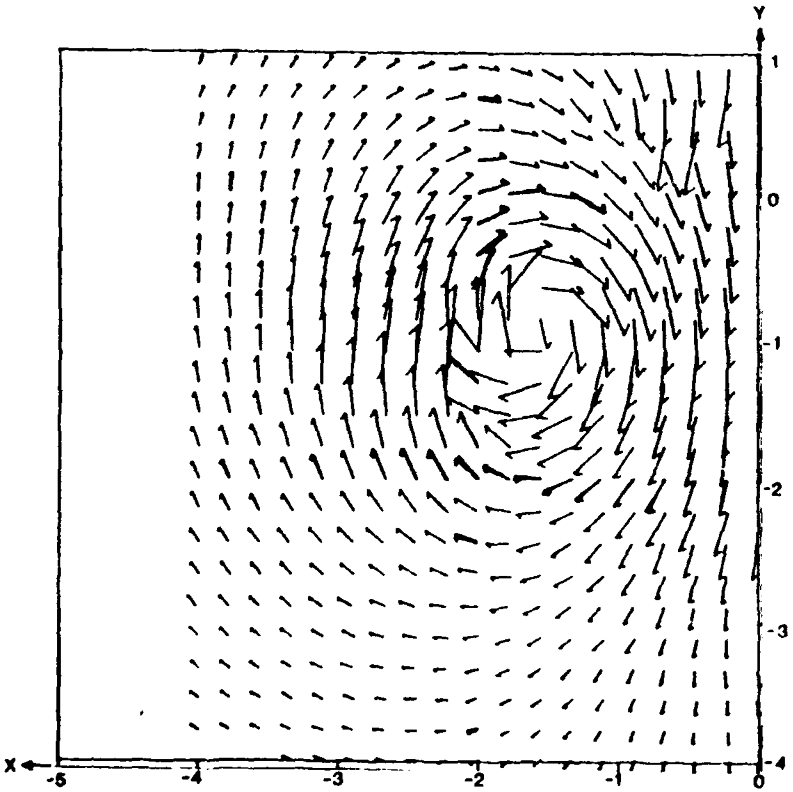

Figure 18. Bent Plate Cross Velocity Vector Plot, α = 10° and 12 Inches Downstream

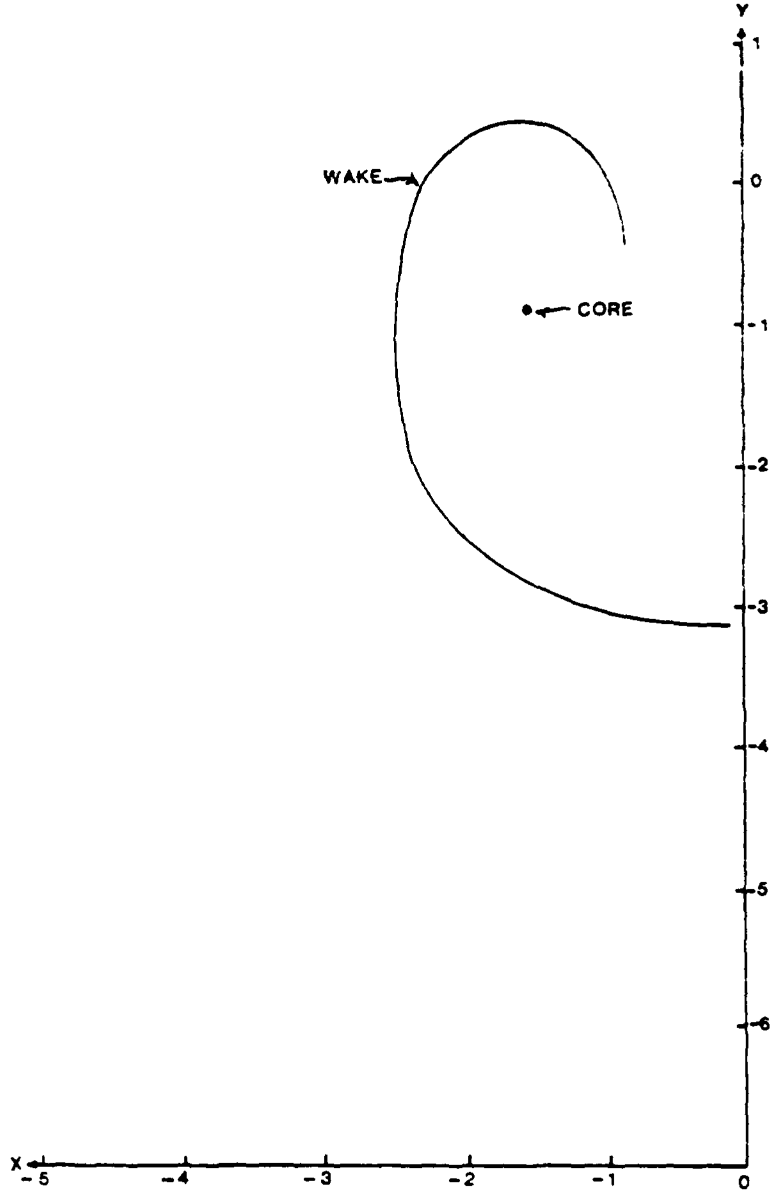

Figure 19. Bent Plate Wake Location, α = 10° and 12 Inches Downstream

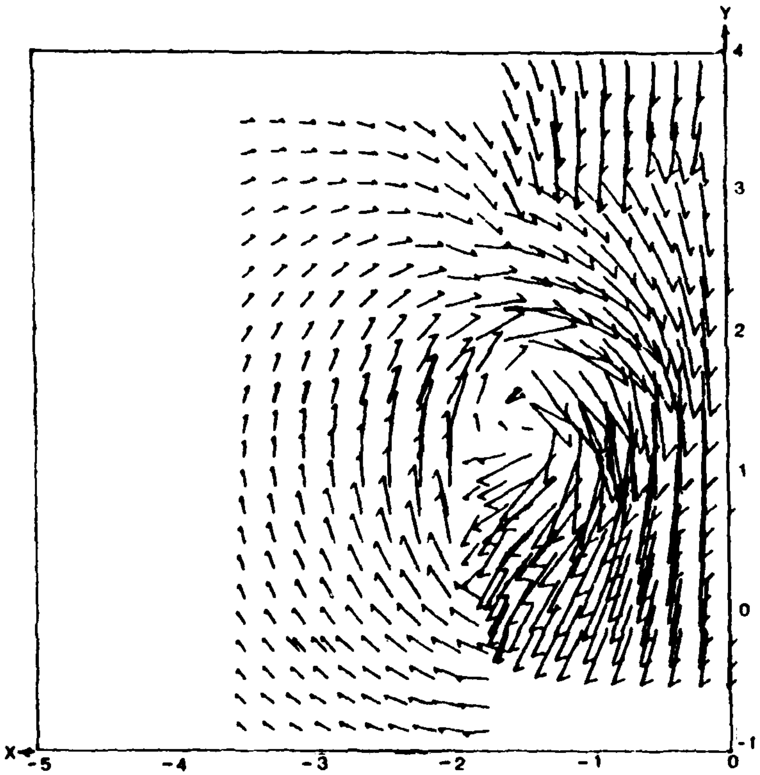

Figure 20. Bent Plate Cross Velocity Vector Plot, α = 20° and 2 Inches Upstream

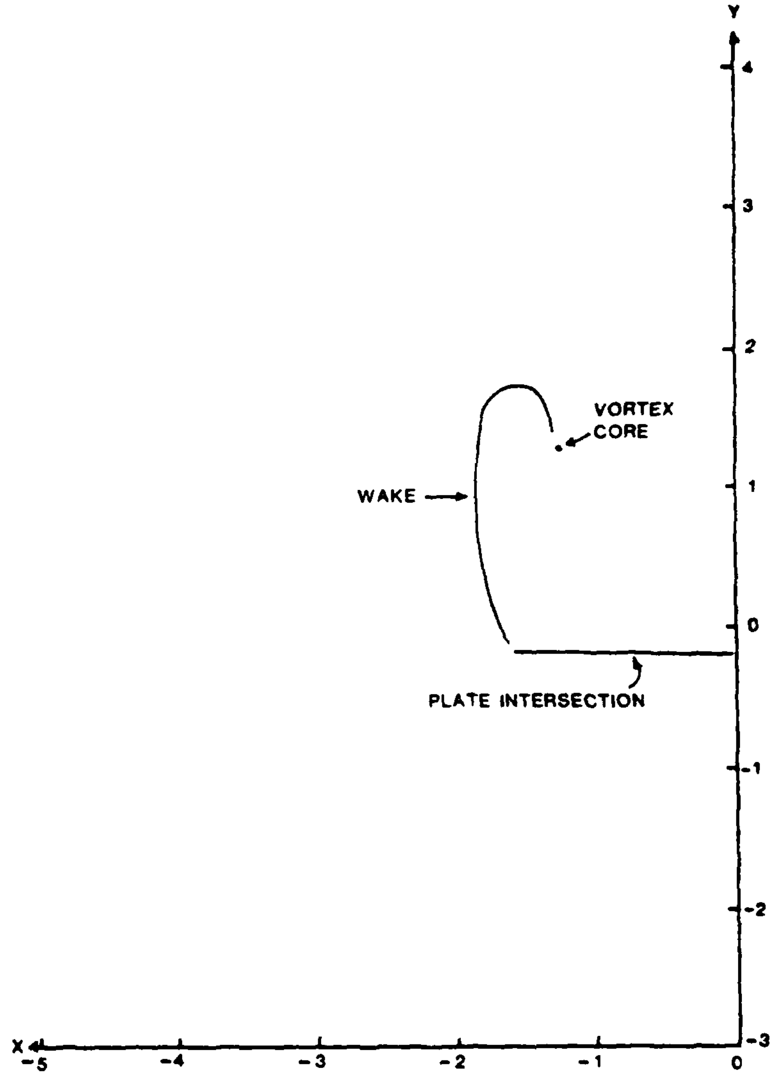

Figure 21. Bent Plate Wake Location, α = 20° and 2 Inches Upstream

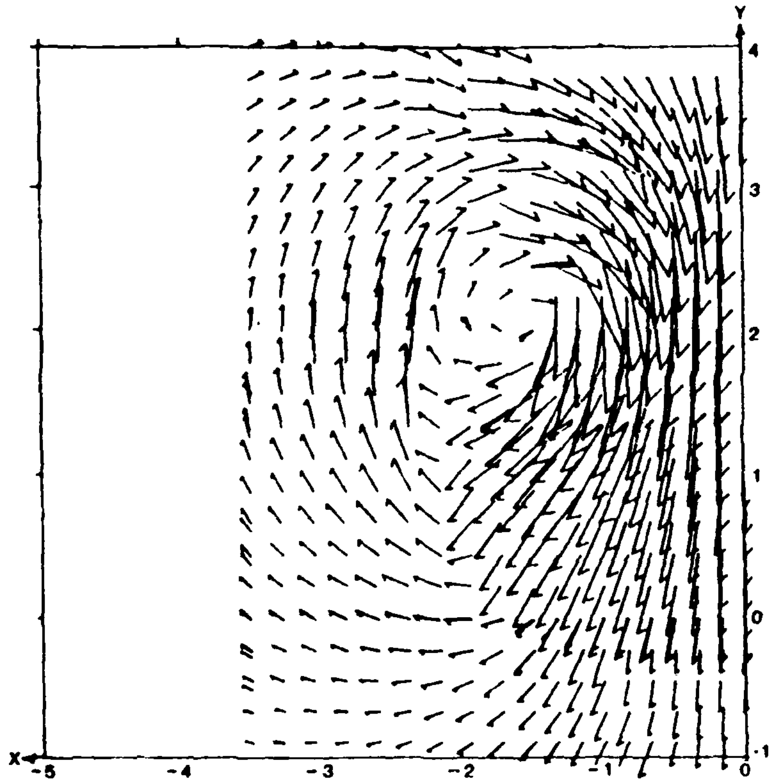

Figure 22. Bent Plate Cross Velocity Vector Plot, α = 20° and .2 Inches Downstream

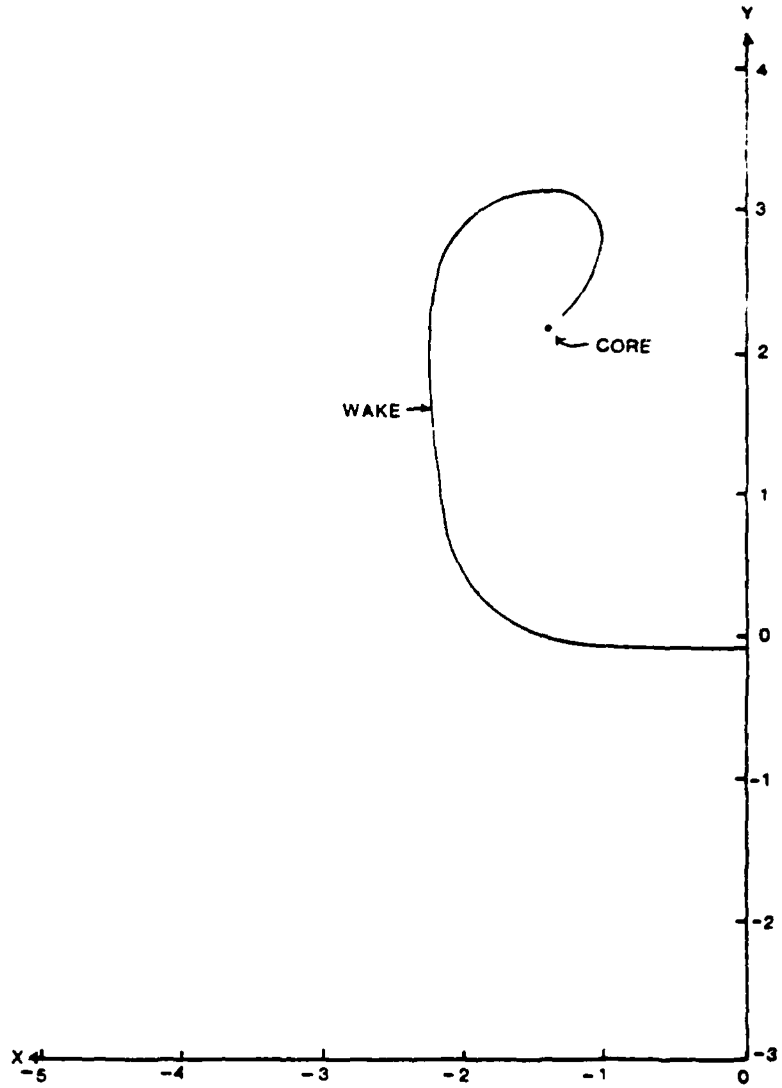

Figure 23. Bent Plate Wake Location, α = 20° and .2 Inches Downstream

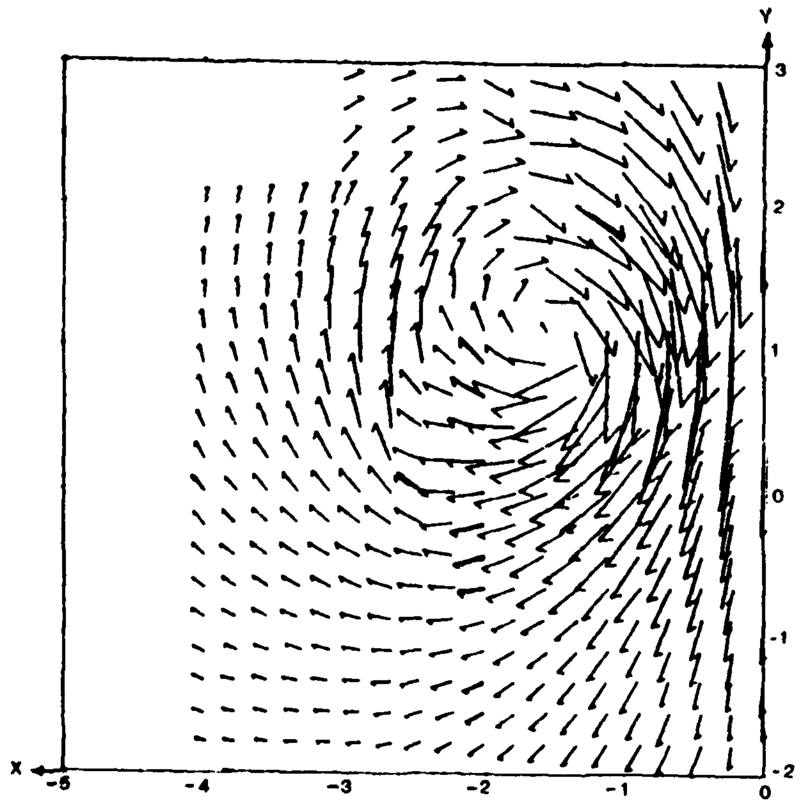

Figure 24. Bent Plate Cross Velocity Vector Plot, $\alpha = 20°$ and 2 Inches Downstream

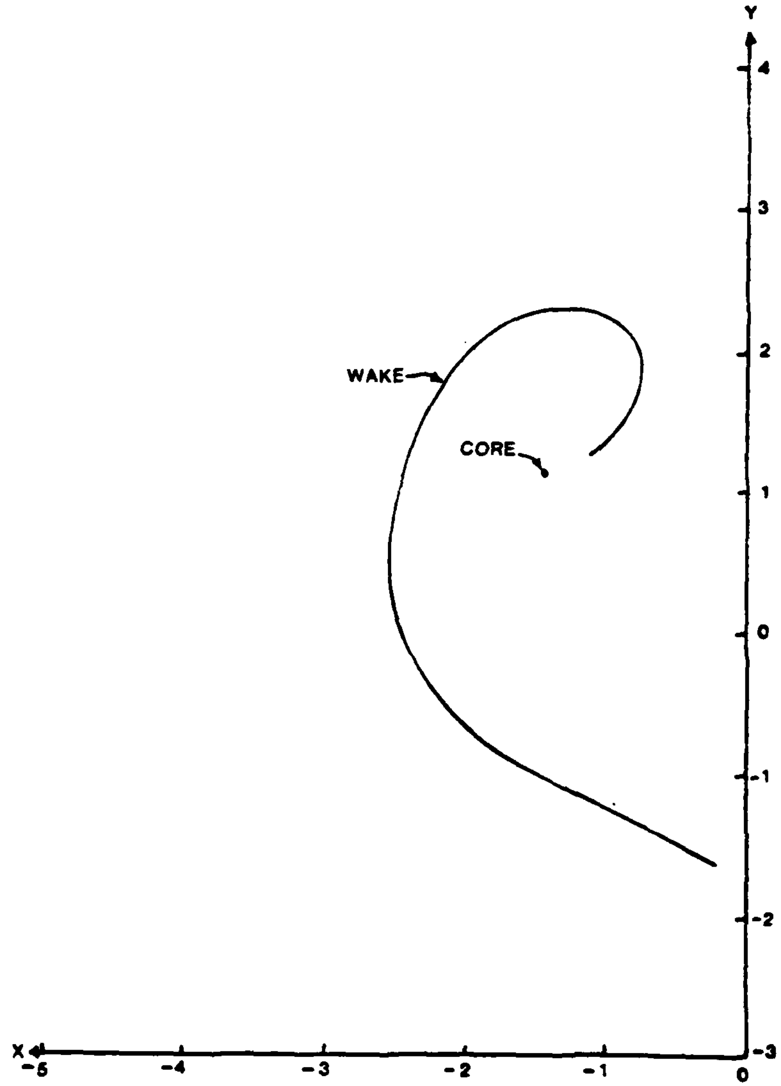

Figure 25. Bent Plate Wake Location, $\alpha = 20°$ and 2 Inches Downstream

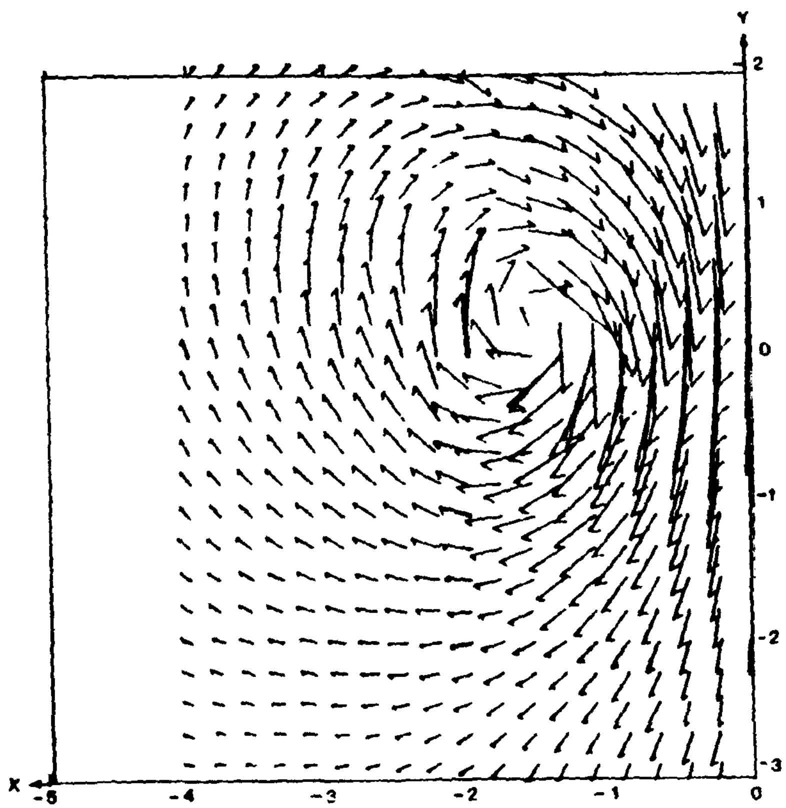

Figure 26. Bent Plate Cross Velocity Vector Plot, $\alpha = 20°$ and 4 Inches Downstream

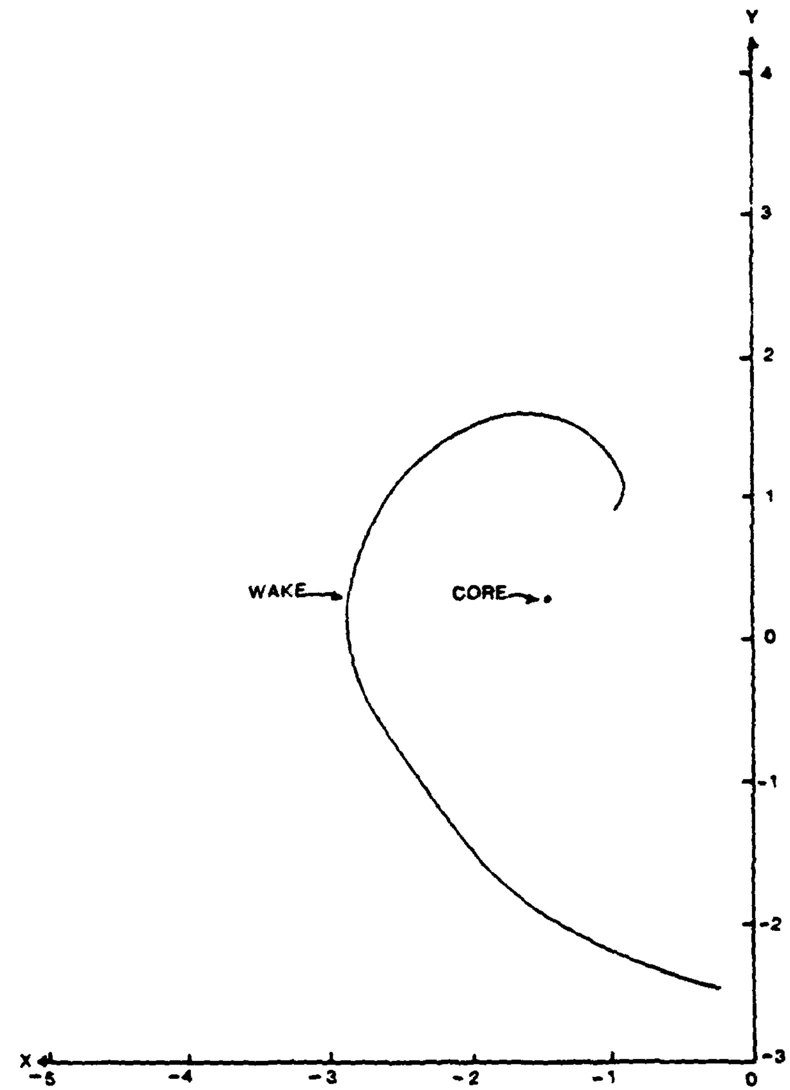

Figure 27. Bent Plate Wake Location, $\alpha = 20°$ and 4 Inches Downstream

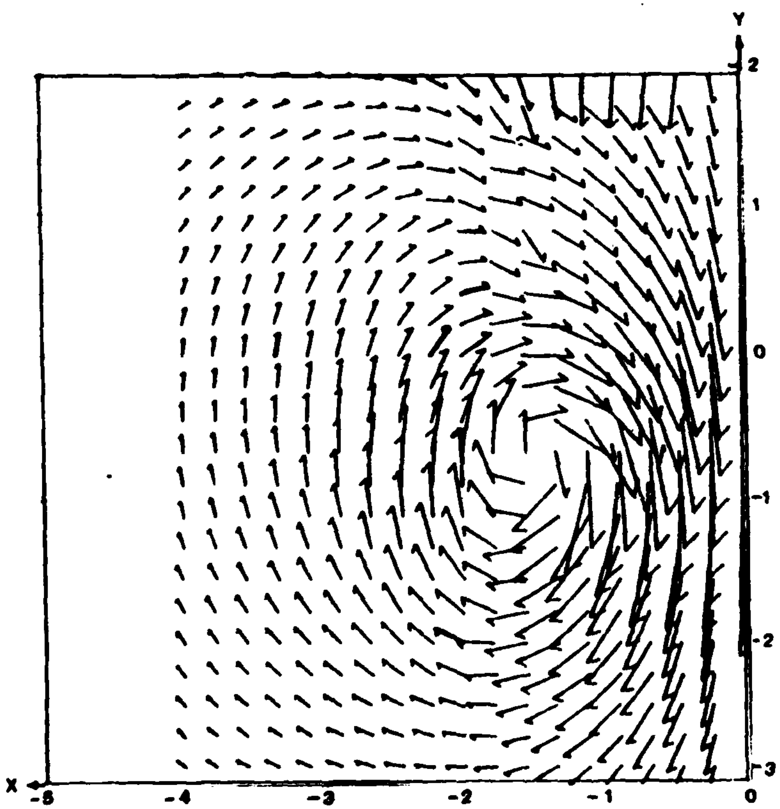

Figure 28. Bent Plate Cross Velocity Vector Plot, $\alpha = 20°$ and 6 Inches Downstream

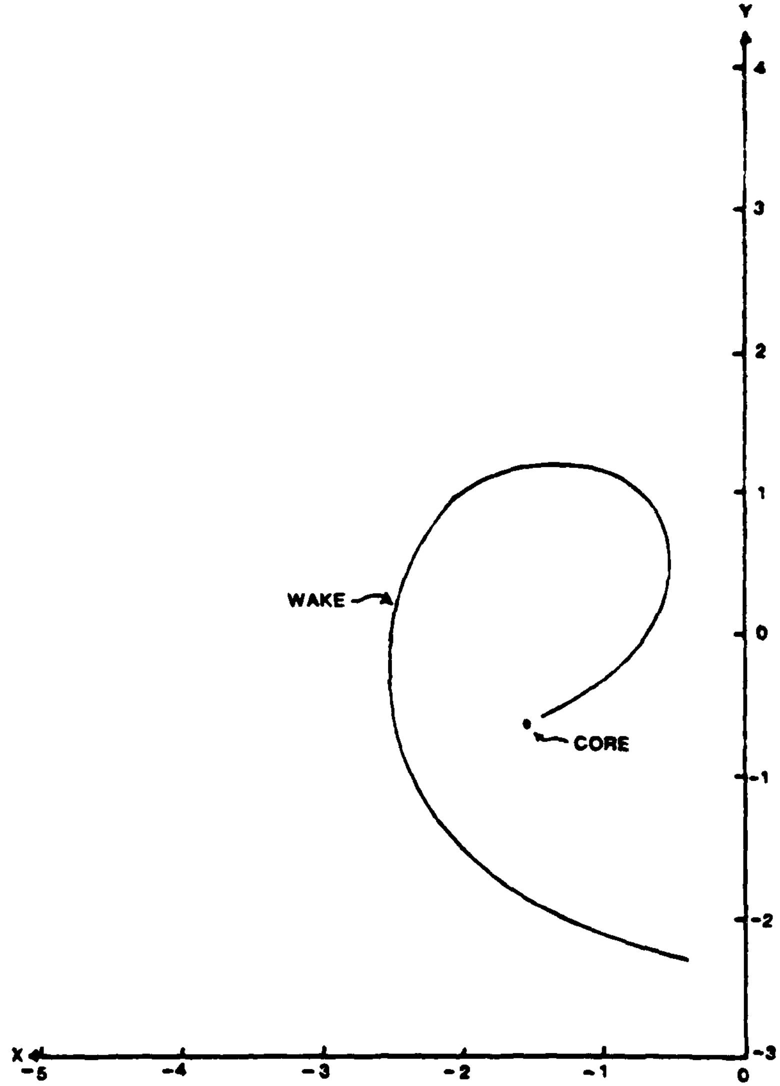

Figure 29. Bent Plate Wake Location, $\alpha = 20°$ and 6 Inches Downstream

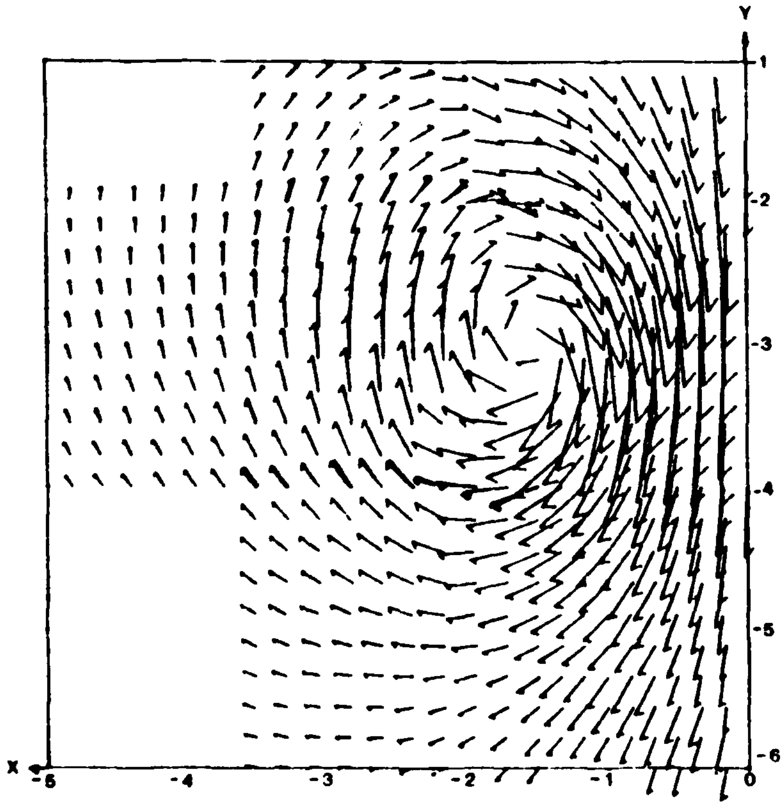

Figure 30. Bent Plate Cross Velocity Vector Plot, α = 20° and 11.5 Inches Downstream

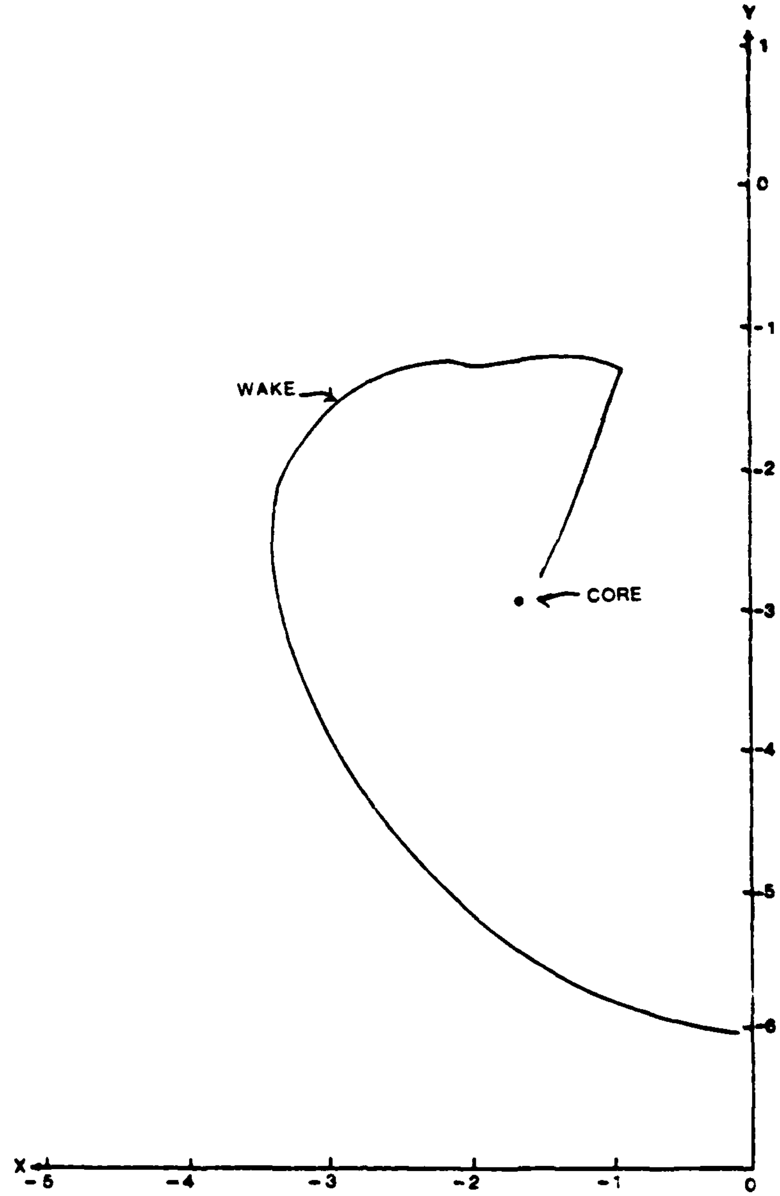

Figure 31. Bent Plate Wake Location, α = 20° and 11.5 Inches Downstream

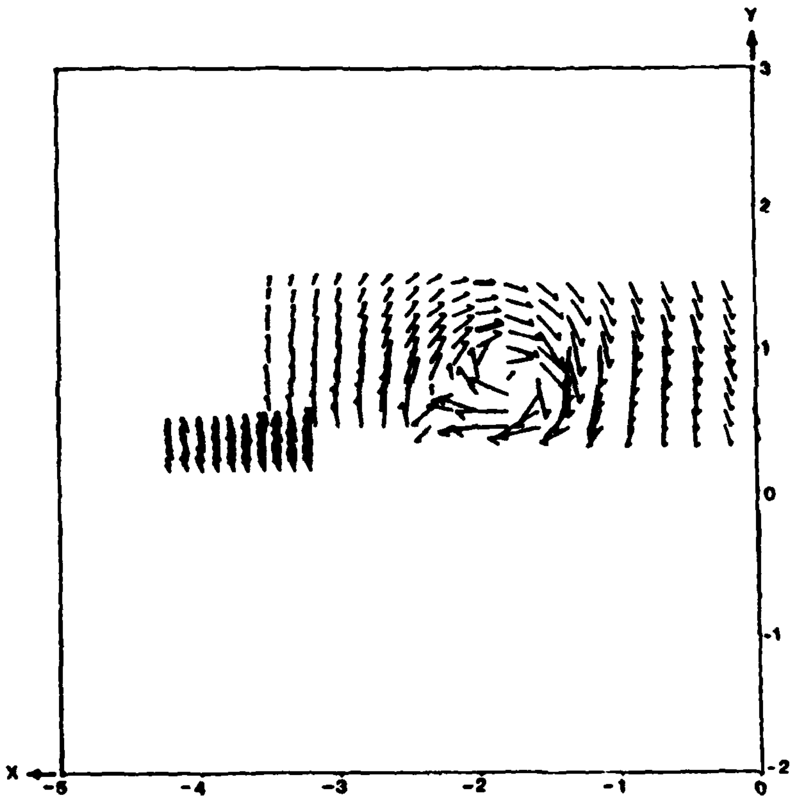

Figure 32. Delta Wing Cross Velocity Vector Plot, $\alpha = 10°$ and 2 Inches Upstream

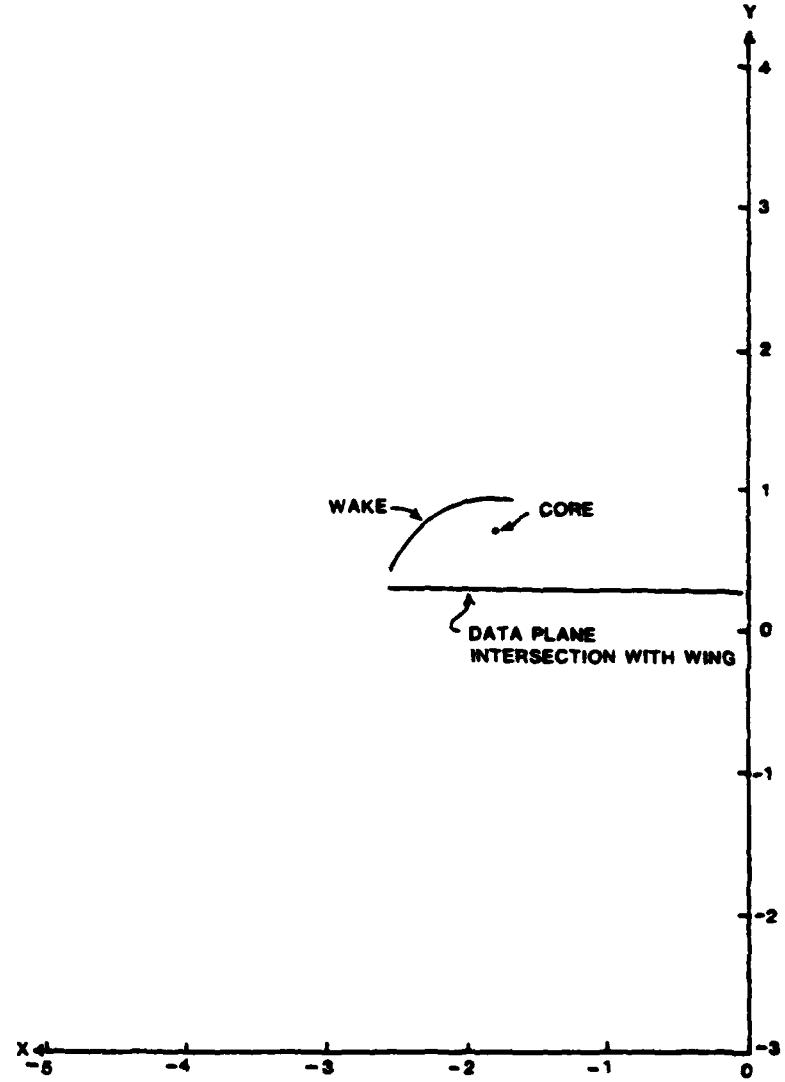

Figure 33. Delta Wing Wake Location, $\alpha = 10°$ and 2 Inches Upstream

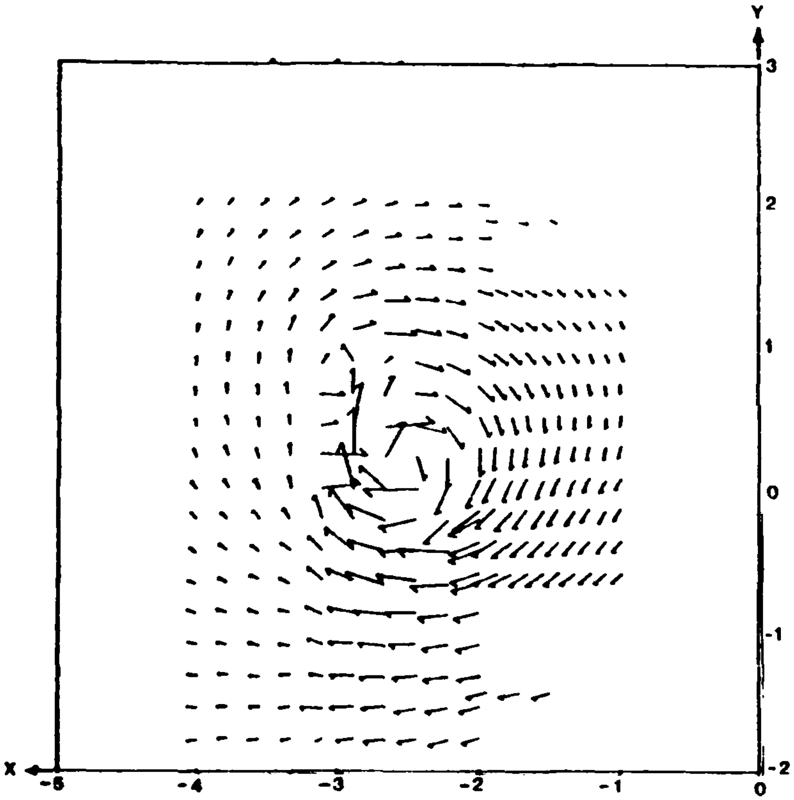

Figure 34. Delta Wing Cross Velocity Vector Plot, α = 10° and .2 Inches Downstream

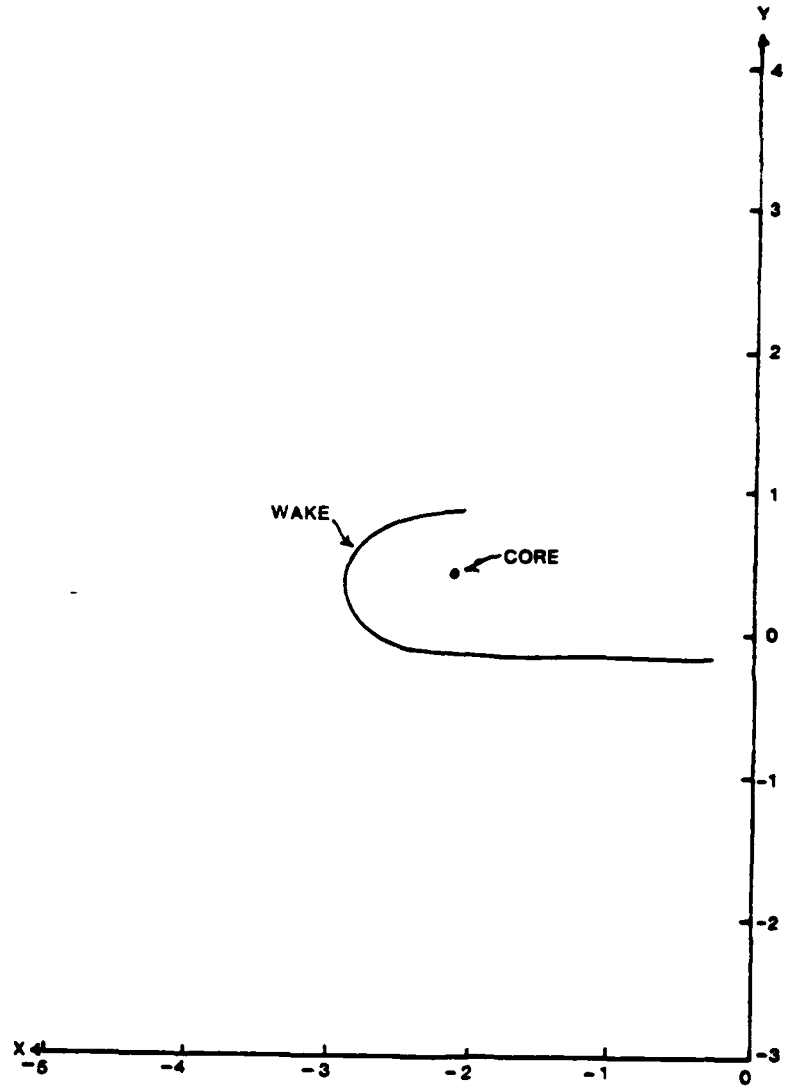

Figure 35. Delta Wing Wake Location, α = 10° and .2 Inches Downstream

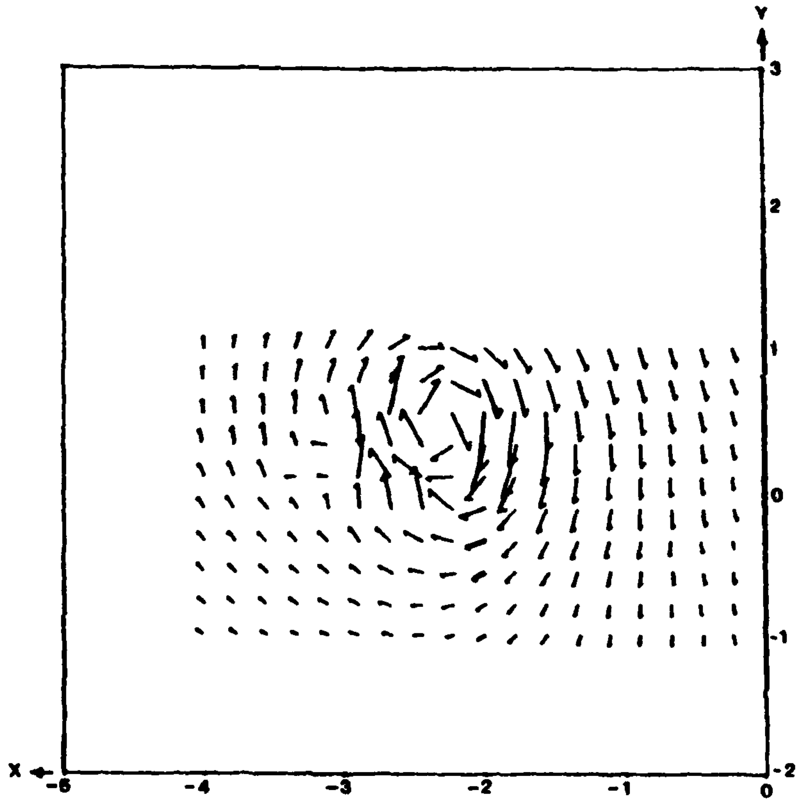

Figure 36. Delta Wing Cross Velocity Vector Plot, $\alpha = 10°$ and 2 Inches Downstream

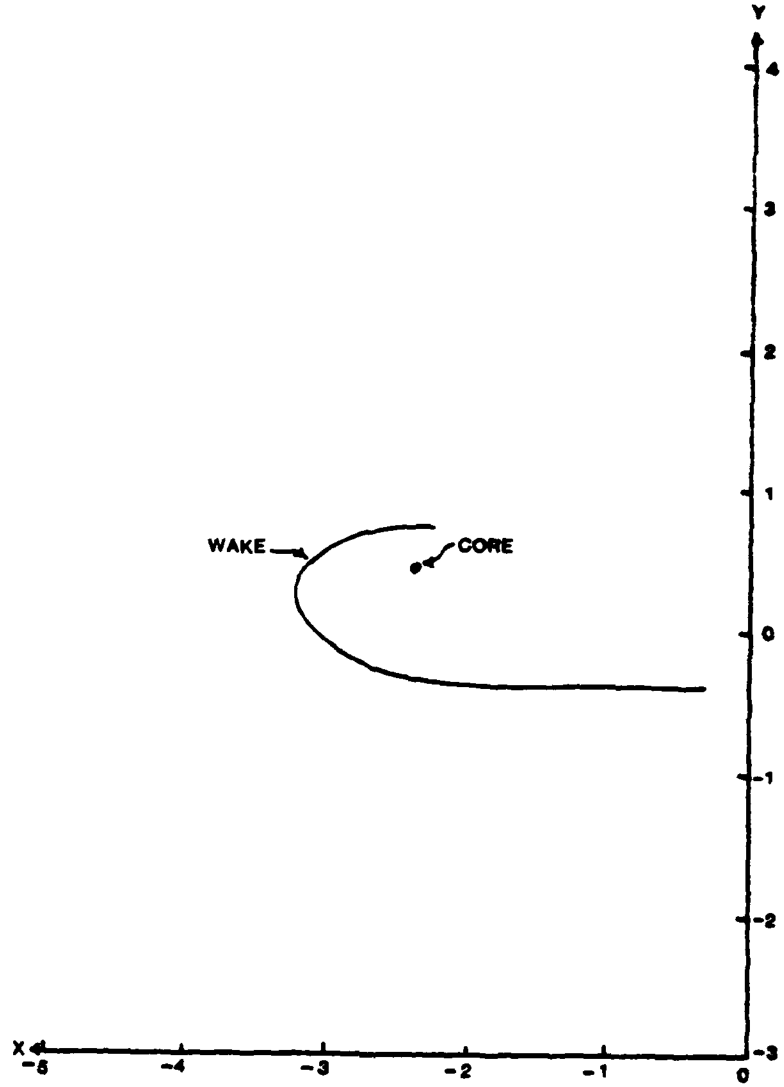

Figure 37. Delta Wing Wake Location $\alpha = 10°$ and 2 Inches Downstream

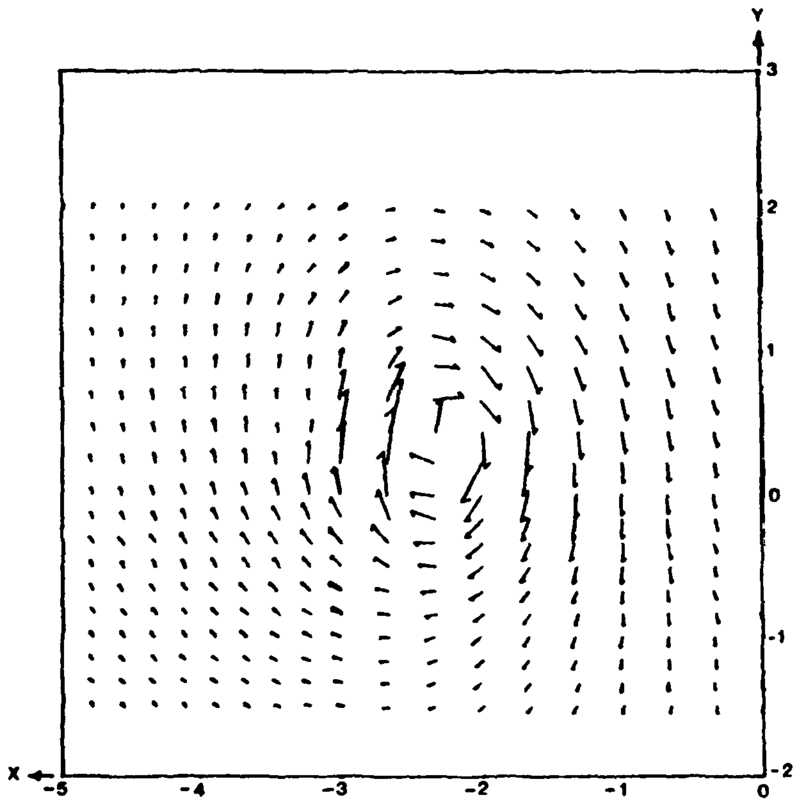

Figure 38. Delta Wing Cross Velocity Vector Plot, α = 10° and 4 Inches Downstream

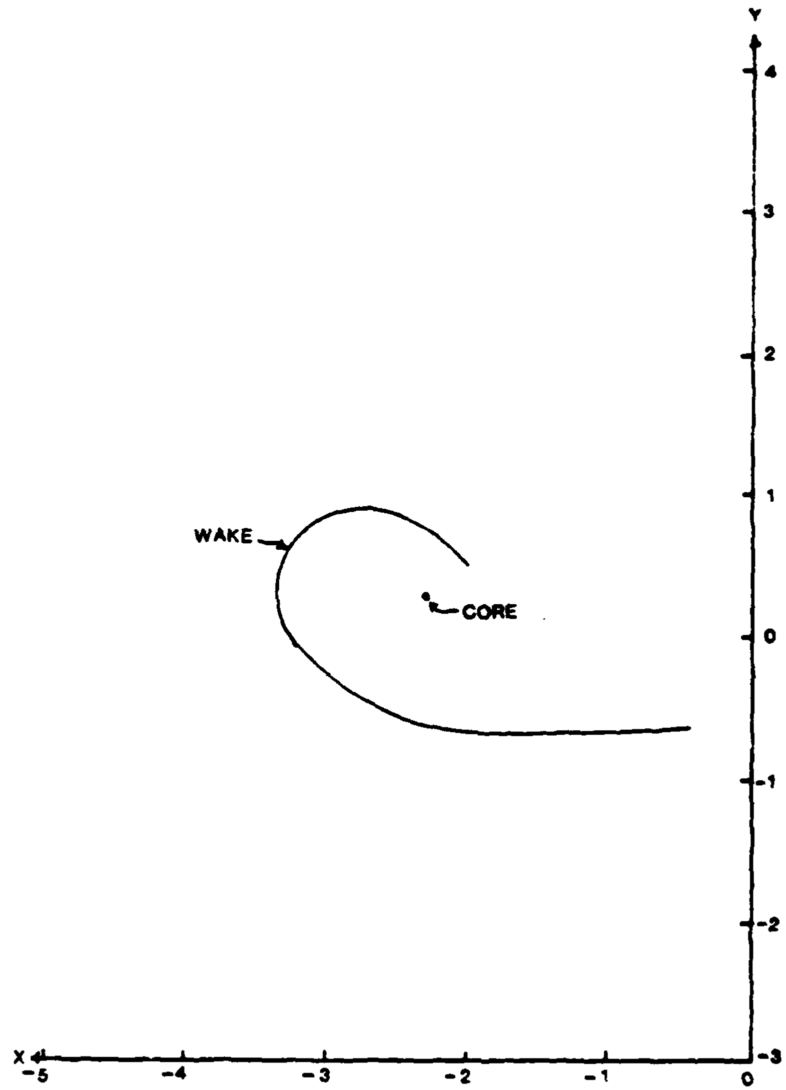

Figure 39. Delta Wing Wake Location α = 10° and 4 Inches Downstream

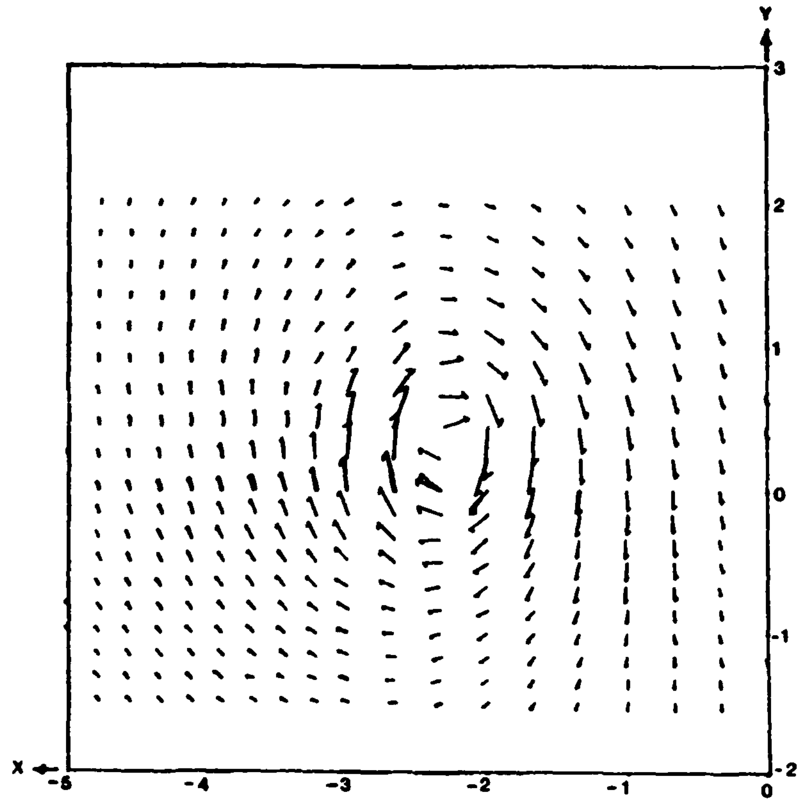

Figure 40. Delta Wing Cross Velocity Vector Plot, α = 10° and 6 Inches Downstream

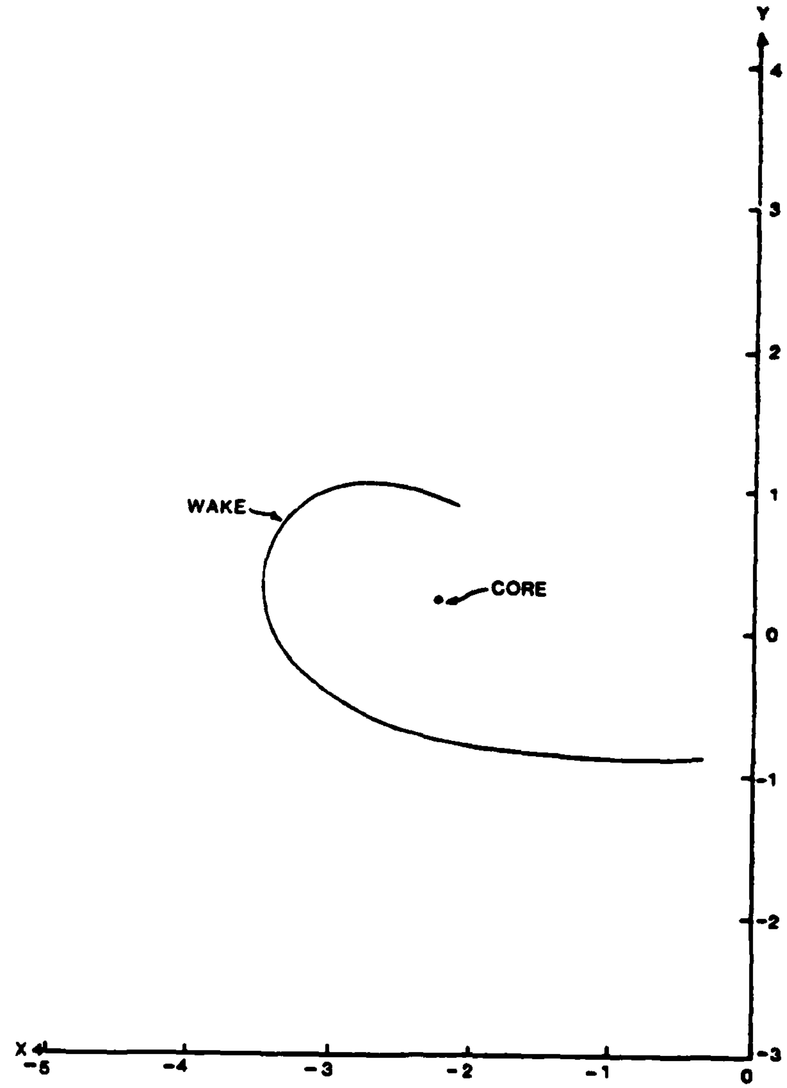

Figure 41. Delta Wing Wake Location α = 10° and 6 Inches Downstream

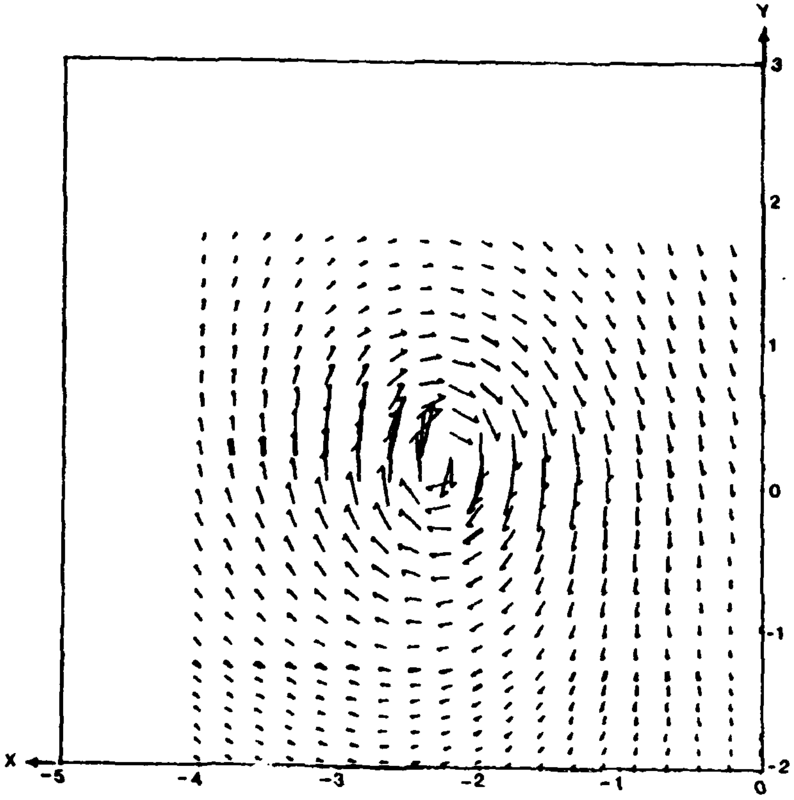

Figure 42. Delta Wing Cross Velocity Vector Plot, α = 10° and 9 Inches Downstream

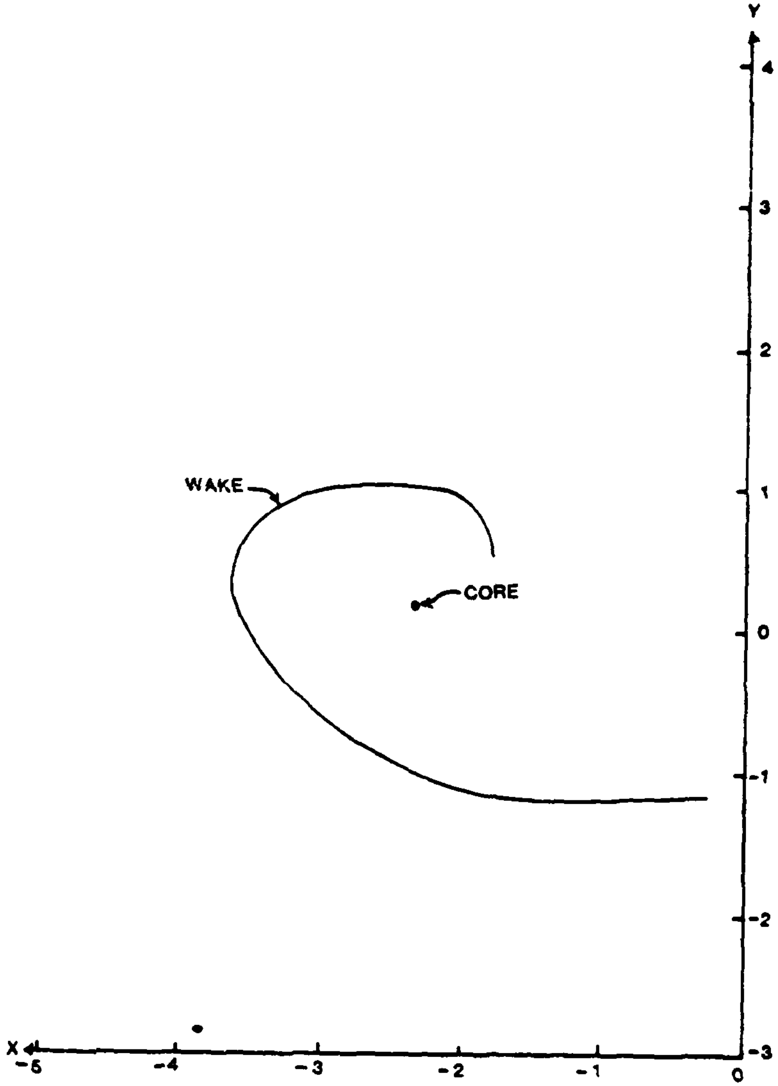

Figure 43. Delta Wing Wake Location α = 10° and 9 Inches Downstream

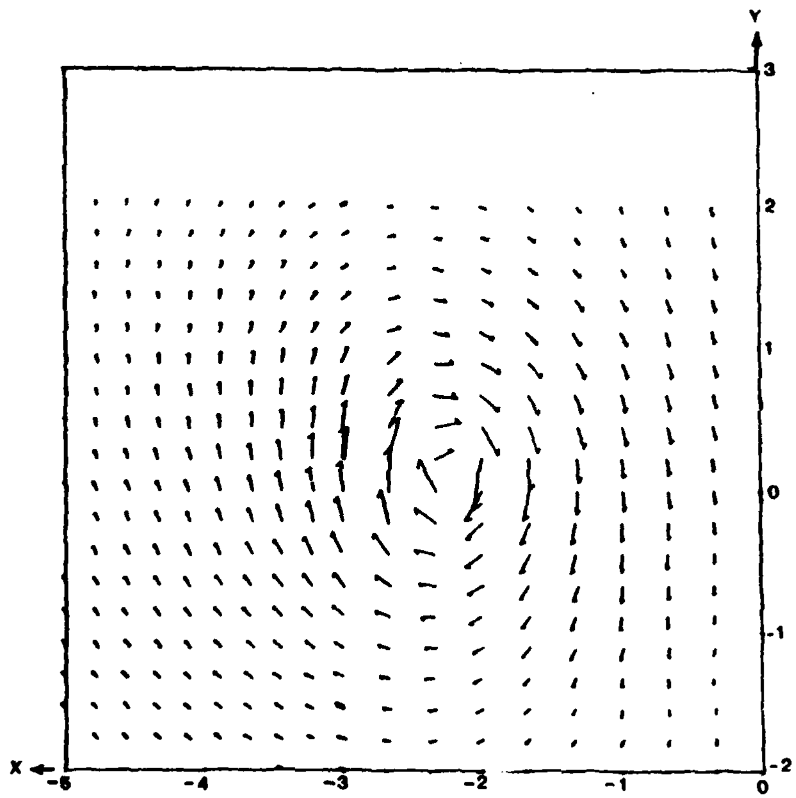

Figure 44. Delta Wing Cross Velocity Vector Plot, $\alpha = 10°$ and 12 Inches Downstream

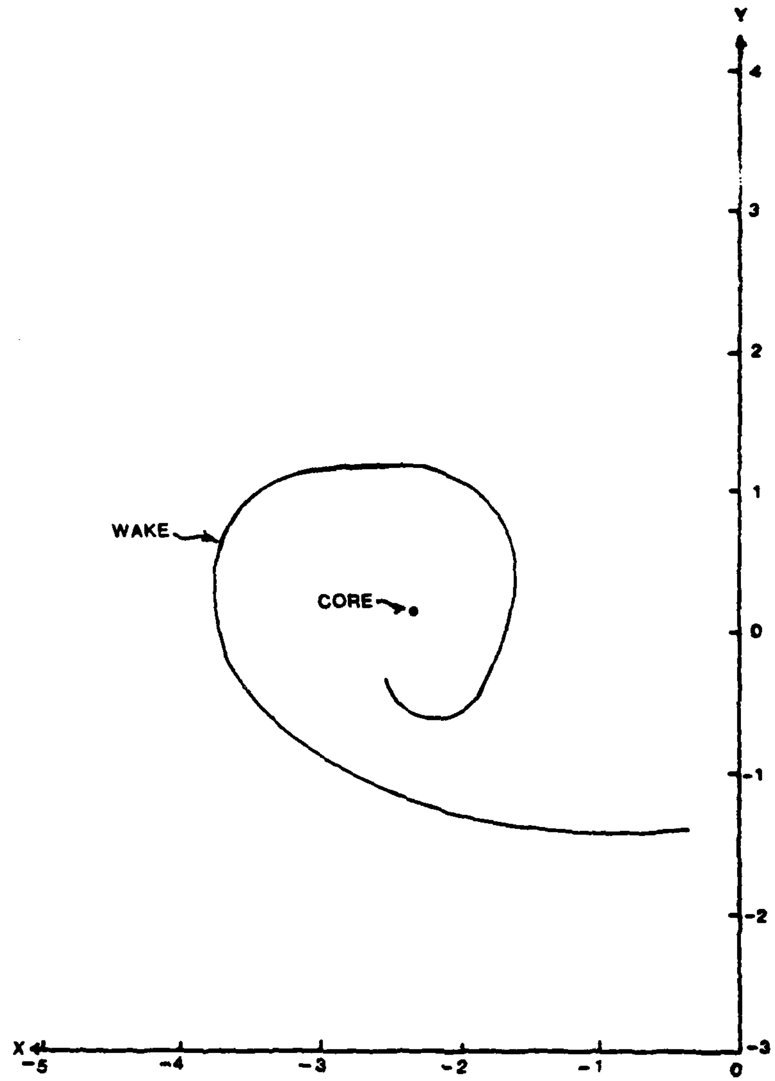

Figure 45. Delta Wing Wake Location $\alpha = 10°$ and 12 Inches Downstream

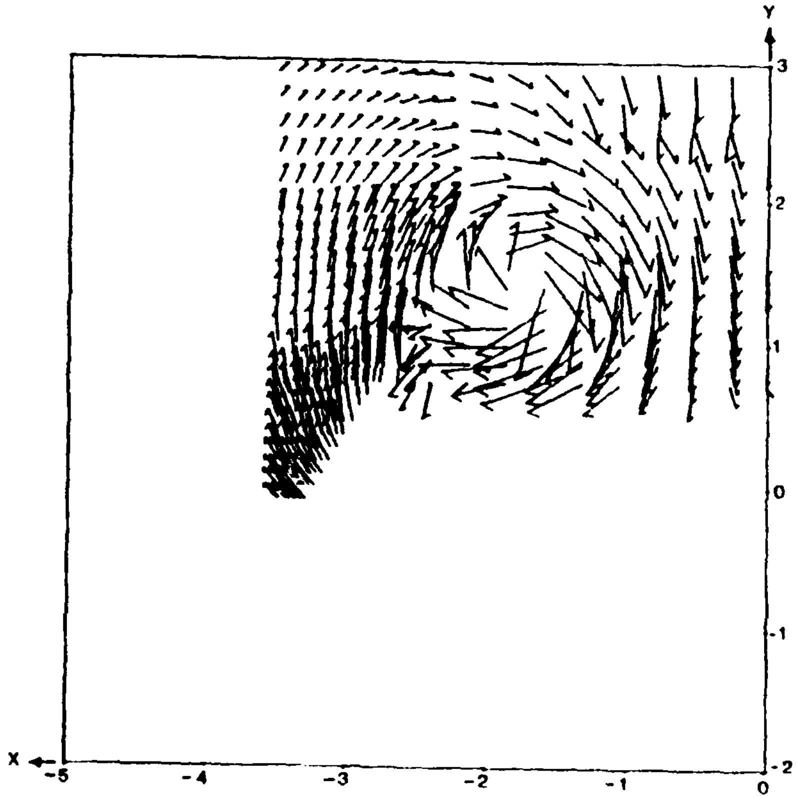

Figure 46. Delta Wing Cross Velocity Vector Plot, $\alpha = 20°$ and 2 Inches Upstream

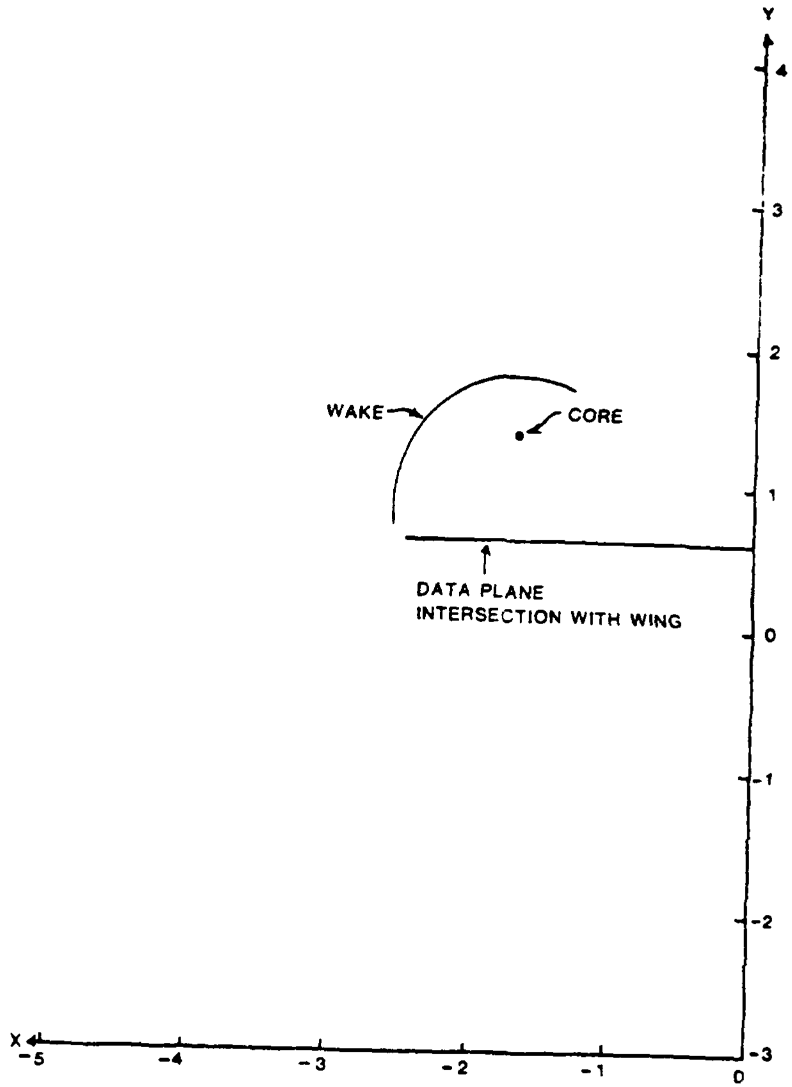

Figure 47. Delta Wing Wake Location $\alpha = 20°$ and 2 Inches Upstream

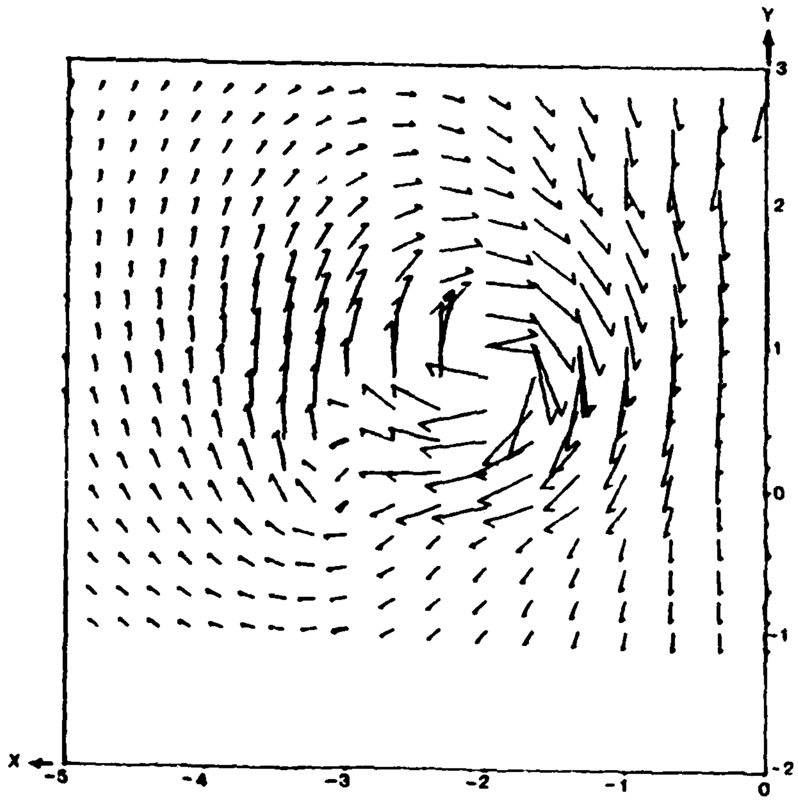

Figure 48. Delta Wing Cross Velocity Vector Plot, $\alpha = 20°$ and .2 *Inches Downstream*

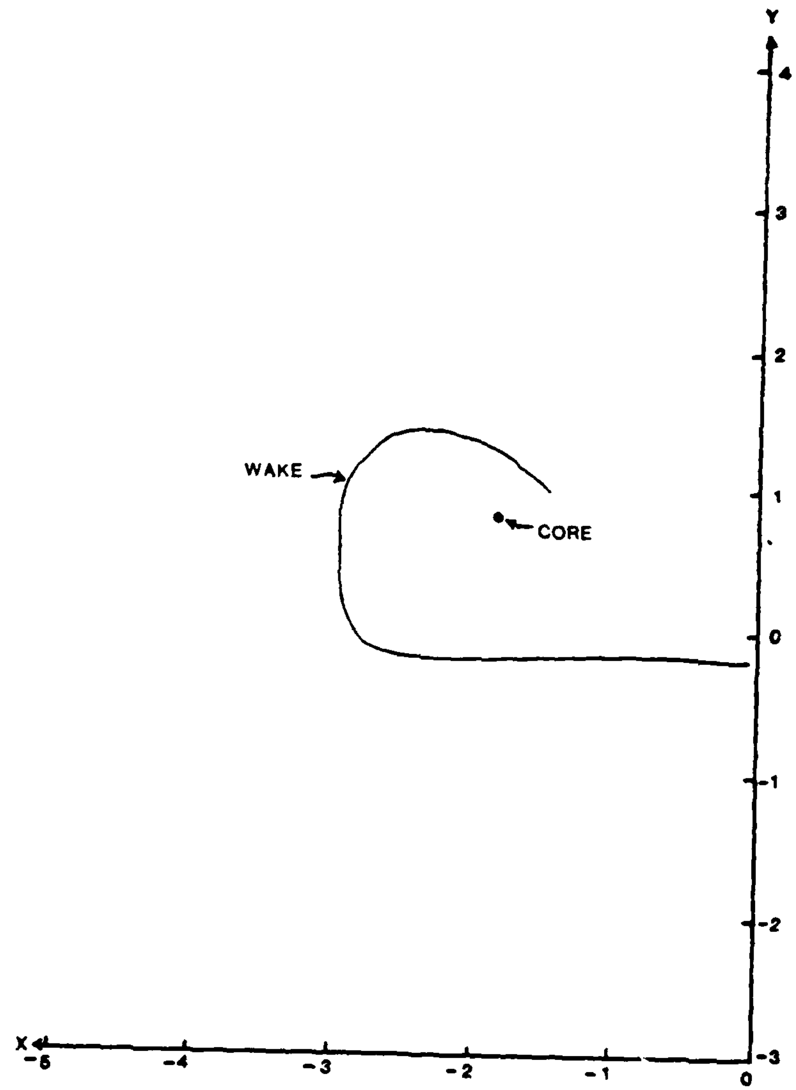

Figure 49. Delta Wing Wake Location $\alpha = 20°$ and .2 Inches Downstream

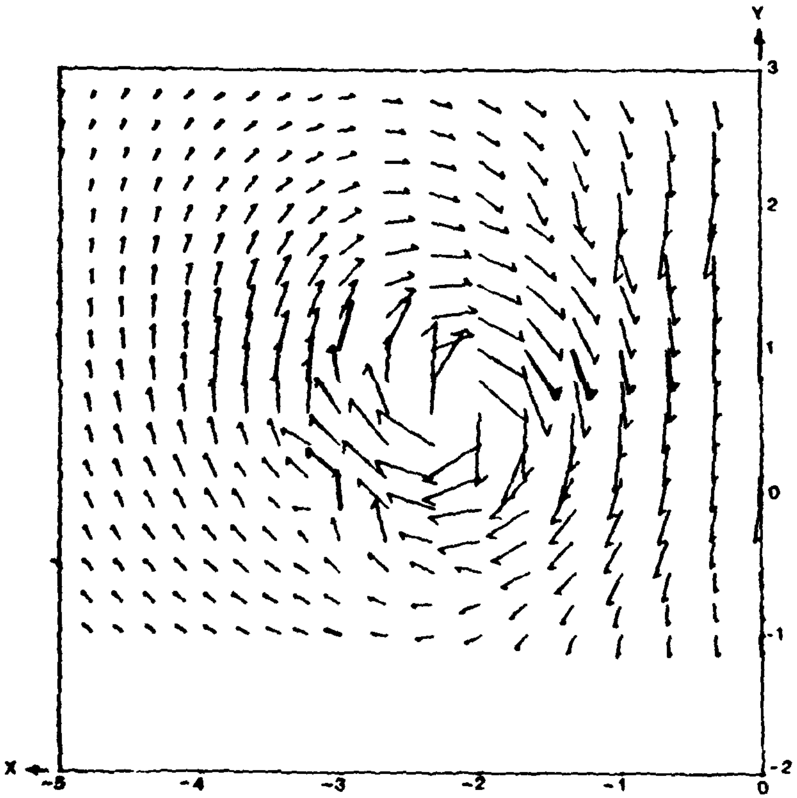

Figure 50. Delta Wing Cross Velocity Vector Plot, α = 20° and 2 Inches Downstream

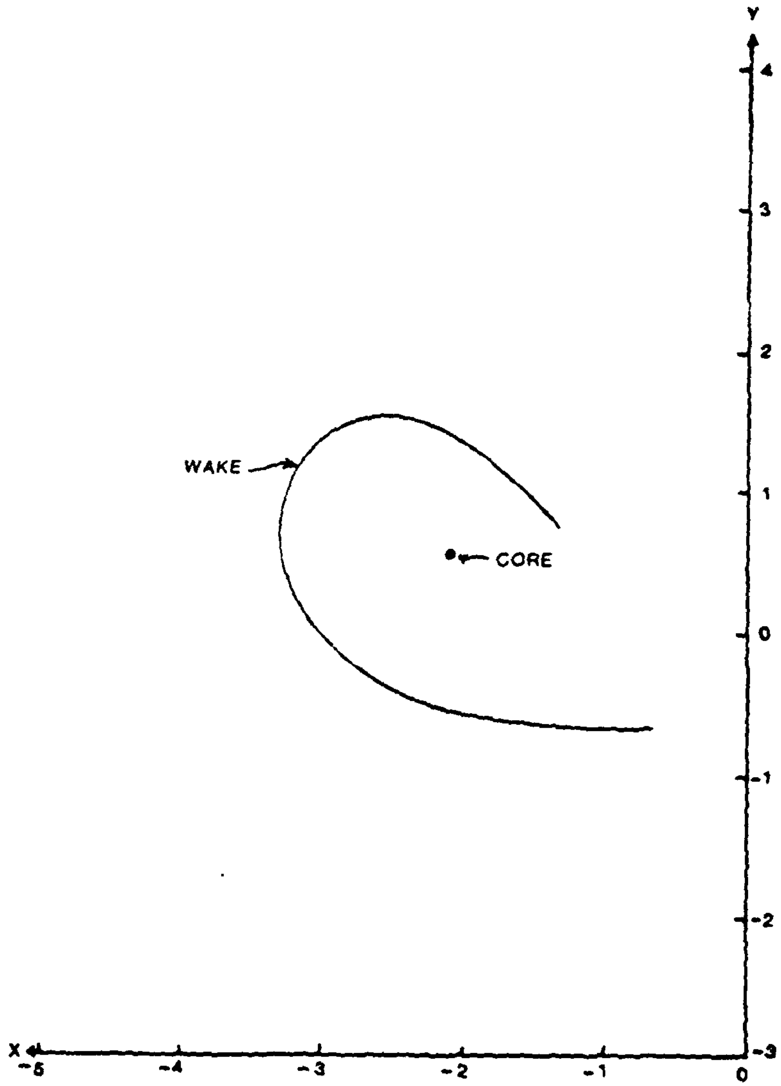

Figure 51. Delta Wing Wake Location α = 20° and 2 Inches Downstream

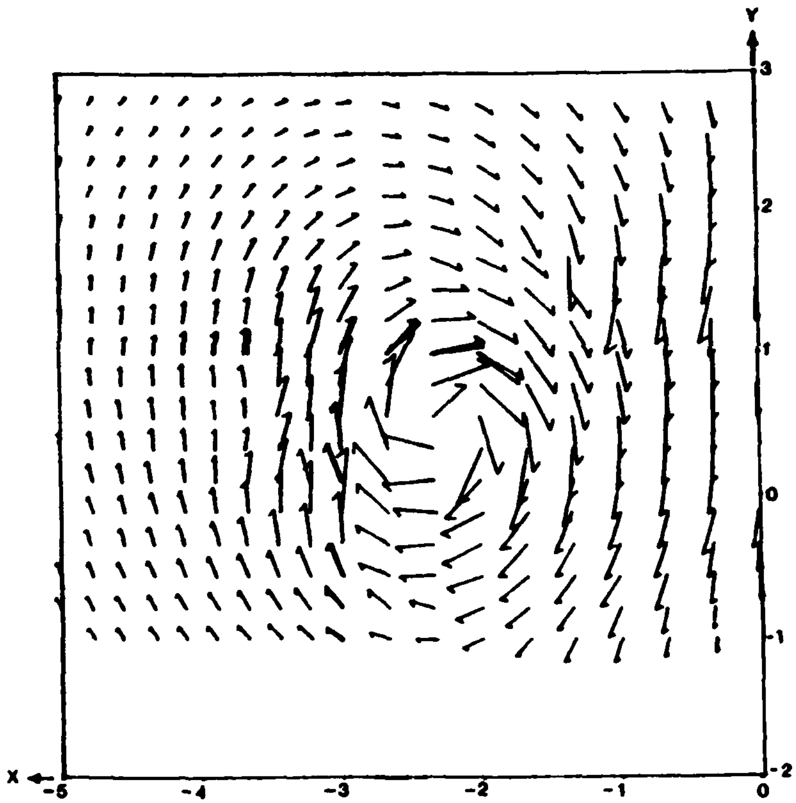

Figure 52. Delta Wing Cross Velocity Vector Plot, $\alpha = 20°$ and 4 Inches Downstream

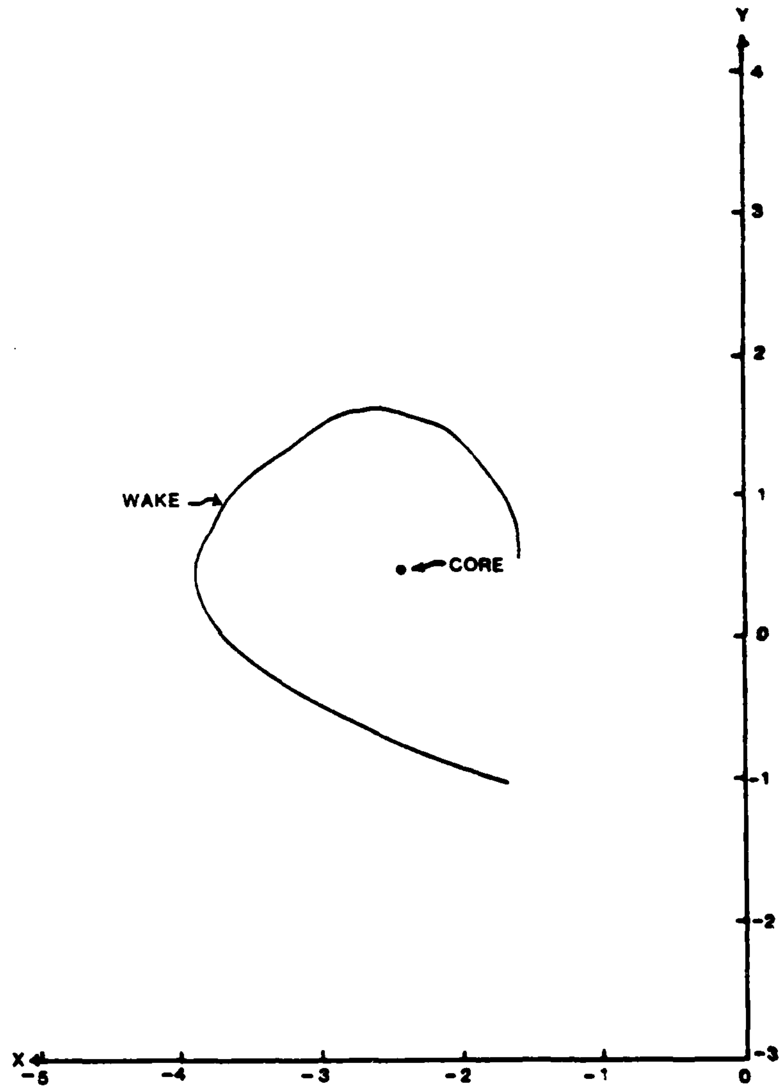

Figure 53. Delta Wing Wake Location $\alpha = 20°$ and 4 Inches Downstream

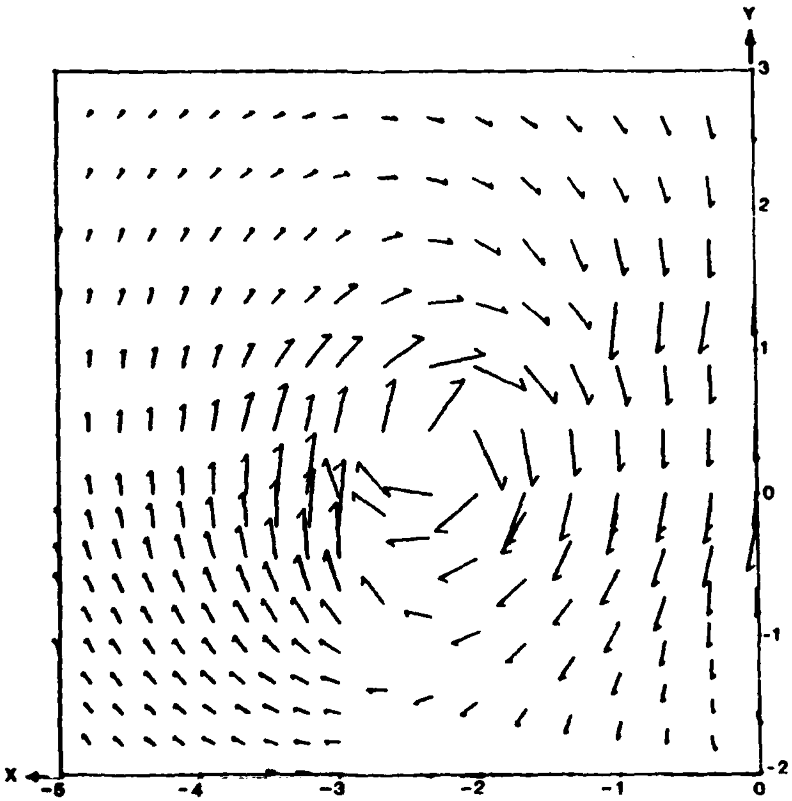

Figure 54. Delta Wing Cross Velocity Vector Plot, α = 20° and 6 Inches Downstream

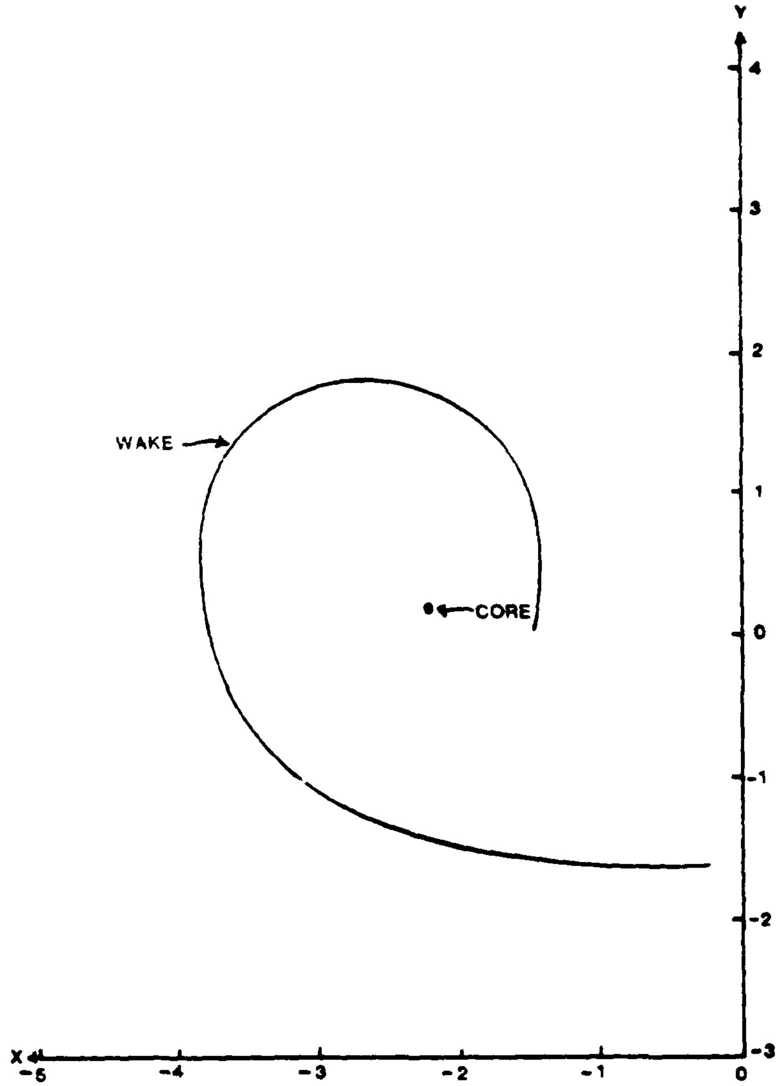

Figure 55. Delta Wing Wake Location α = 20° and 6 Inches Downstream

END

DATE
FILMED

8-83

DTIC